AD-A172 326 CERENKOV RADIATION: TIME DEPENDENT B FIELD OVER A FINITE PATH(U) NAVAL POSTGRADUATE SCHOOL MONTEREY CA K M LYMAN JUN 86 1/1

UNCLASSIFIED F/G 20/8 NL

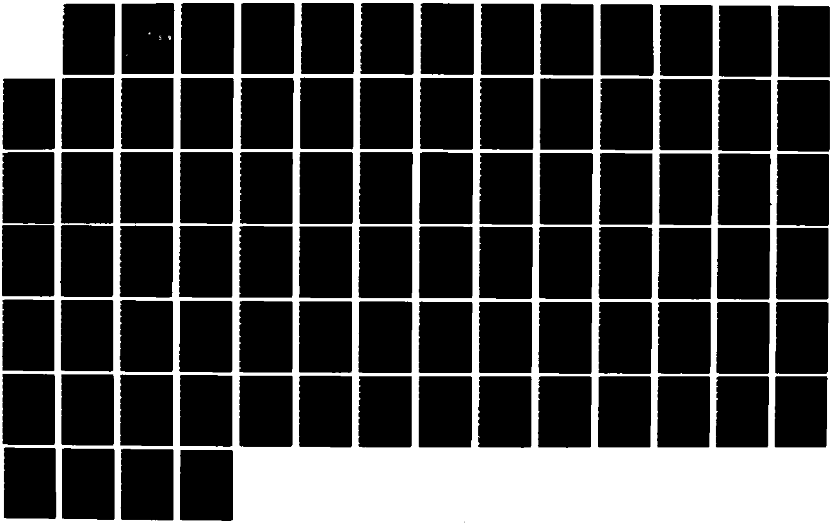

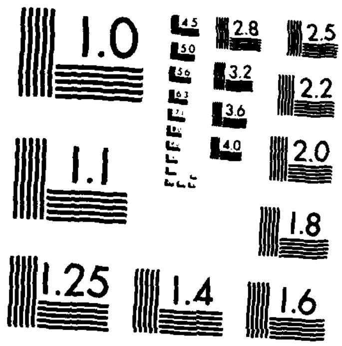
1.0
1.1
1.25
1.4
1.6
1.8
2.0
2.2
2.5
2.8
3.2
3.6
4.0

AD-A172 326

DTIC FILE COPY

NAVAL POSTGRADUATE SCHOOL

Monterey, California

DTIC ELECTE OCT 0 1 1986 S D

D

THESIS

CERENKOV RADIATION: TIME DEPENDENT
B FIELD OVER A FINITE PATH

by

Kathleen Marie Lyman

June 1986

Thesis Advisor: John R. Neighbours

Approved for public release; distribution is unlimited

86 10 01 044

SECURITY CLASSIFICATION OF THIS PAGE

AD-A172 326

REPORT DOCUMENTATION PAGE

1a REPORT SECURITY CLASSIFICATION Unclassified	1b RESTRICTIVE MARKINGS
2a SECURITY CLASSIFICATION AUTHORITY	3 DISTRIBUTION/AVAILABILITY OF REPORT Approved for public release; distribution is unlimited
2b DECLASSIFICATION/DOWNGRADING SCHEDULE	
4 PERFORMING ORGANIZATION REPORT NUMBER(S)	5 MONITORING ORGANIZATION REPORT NUMBER(S)
6a NAME OF PERFORMING ORGANIZATION Naval Postgraduate School 6b OFFICE SYMBOL (If applicable) 33	7a NAME OF MONITORING ORGANIZATION Naval Postgraduate School
6c ADDRESS (City, State, and ZIP Code) Monterey, California 93943-5100	7b ADDRESS (City, State, and ZIP Code) Monterey, California 93943-5100
8a NAME OF FUNDING/SPONSORING ORGANIZATION 8b OFFICE SYMBOL (If applicable)	9 PROCUREMENT INSTRUMENT IDENTIFICATION NUMBER
8c ADDRESS (City, State, and ZIP Code)	10 SOURCE OF FUNDING NUMBERS PROGRAM ELEMENT NO / PROJECT NO / TASK NO / WORK UNIT ACCESSION NO

11 TITLE (Include Security Classification)
Cerenkov Radiation: Time Dependent B Field Over a Finite Path

12 PERSONAL AUTHOR(S)
Kathleen M. Lyman

13a TYPE OF REPORT	13b TIME COVERED	14 DATE OF REPORT (Year, Month, Day)	15 PAGE COUNT
Masters Thesis	FROM ______ TO ______	1986, June	85

16 SUPPLEMENTARY NOTATION

17 COSATI CODES			18 SUBJECT TERMS (Continue on reverse if necessary and identify by block number)
FIELD	GROUP	SUB-GROUP	Cerenkov Radiation, Magnetic Field, Finite Path, Time

19 ABSTRACT (Continue on reverse if necessary and identify by block number)

This preliminary study investigated the magnetic field radiated from a passing charge bunch traveling over a finite path. Beginning with the infinite path case for a ramp front charge distribution, limits were derived to solve for the magnetic radiation field over a finite path. Radiation pulses were computed and graphed for many different positions of an observer with respect to the beam line. Comparisons of results show that the similarity in pulse shapes does not depend exclusively on the observer's position with respect to the Cerenkov region, but also on certain time conditions in each case.

20 DISTRIBUTION/AVAILABILITY OF ABSTRACT ☒ UNCLASSIFIED/UNLIMITED ☐ SAME AS RPT ☐ DTIC USERS	21 ABSTRACT SECURITY CLASSIFICATION Unclassified	
22a NAME OF RESPONSIBLE INDIVIDUAL John R. Neighbours	22b TELEPHONE (Include Area Code) (408) 646-2922	22c OFFICE SYMBOL 61Nb

DD FORM 1473, 84 MAR — 83 APR edition may be used until exhausted. All other editions are obsolete.

SECURITY CLASSIFICATION OF THIS PAGE

Approved for public release; distribution is unlimited.

Cerenkov Radiation: Time Dependent B Field Over a Finite Path

by

Kathleen Marie Lyman
Lieutenant Commander, United States Navy
B.A., Fordham University, 1970
M.S.T., Fordham University, 1974

Submitted in partial fulfillment of the requirements for the degree of

MASTER OF SCIENCE IN ENGINEERING SCIENCE

from the

NAVAL POSTGRADUATE SCHOOL
June 1986

Author: Kathleen M. Lyman
Kathleen Marie Lyman

Approved by: John R. Neighbours
J.R. Neighbours, Thesis Advisor

Fred R Buskirk
F.R. Buskirk, Second Reader

G E Schacher
Gordon E. Schacher, Chairman, Department of Physics

J.N. Dyer
John N. Dyer, Dean of Science and Engineering

ABSTRACT

This preliminary study investigated the magnetic field radiated from a passing charge bunch traveling over a finite path. Beginning with the infinite path case for a ramp front charge distribution, limits were derived to solve for the magnetic radiation field over a finite path. Radiation pulses were computed and graphed for many different positions of an observer with respect to the beam line. Comparisons of results show that the similarity in pulse shapes does not depend exclusively on the observer's position with respect to the Cerenkov region, but also on certain time conditions in each case.

ses

TABLE OF CONTENTS

I. INTRODUCTION

A. HISTORY

Observations of a bluish-white light near a strong radioactive source had been recorded by workers before this phenomenon was understood. This was during a time (circa 1910) when the electromagnetic theory of light was well known and there was increased study in the area of optics and luminesence. The study of phosphoresence and fluoresence dominated, and the discovery of Cerenkov radiation was postponed due to the complexity of these forms of luminesence and the fact that Cerenkov radiation was weak in comparison. However, eventually the work on Cerenkov radiation developed, and was brought about through the study of phosphoresence and fluoresence. [Ref.1: p.1]

In 1926, Mallet took the first steps to study this phenomenon. He discovered that when a transparent material is placed near a strong radioactive source, the same bluish-white light would be emitted in a wide variety of cases. This light spectrum was continuous and did not contain the line spectrum characteristics of fluoresence. He also discovered that it differed in other respects from other forms of luminesence. The study of the phenomenon was not pursued again until 1934, when Cerenkov began a series of experiments which lasted until 1938. During this same time, Frank and Tamm proposed their theory (1937); there

was excellent correlation between this theory and Cerenkov's experimental results. [Ref.1: pp. 1-2]

Research in this area continued and with the development of the photomultiplier, the study in this area became more active. [Ref.1: p. 2]

B. CERENKOV EFFECT

If a fast moving electron passes through a transparent medium, the atoms around the electron will become distorted and polarized. If the speed of the electron approaches that of light in the medium, then the polarization field is not symmetric. Symmetry is preserved in the azimuthal plane, "but along the axis there is a resultant dipole field which will be apparent even at large distances from the track of the electron." [Ref.1: p. 4] Because of this field, each element along the electron track will radiate a brief electromagnetic pulse. [Ref.1: p. 4]

Generally, these radiated wavelets from all parts of the track will interfere destructively and there will be no resultant field. However, if the particle velocity is higher than the phase velocity of light in the medium, the wavelets will be in phase and there will be a resultant field at a distant point of observation. This is observed only at a particular angle θ with respect to the particle path. [Ref.1: p. 5]

Figure 1 [Ref.1: p. 5] illustrates the coherence of the

wavelets formed from points P_1, P_2, and P_3. If βc_0 is the particle velocity, where c_0 is the speed of light in a vacuum and n is the index of refraction and $\Delta\tau$ is time, then $AB = (\beta c_0)(\Delta\tau)$, the distance traveled by the particle, and $AC = (c_0/n)(\Delta\tau)$, the distance traveled by light. Thus, we can obtain $\cos\theta = 1/\beta n$, which is called the "Cerenkov relation". [Ref.1: p. 5]

There exists a threshold velocity, determined by the relation $\beta_{min} = (1/n)$, and below this, no radiation is emitted. When radiation is emitted, it occurs in the visible and the near visible. [Ref.1: p. 5-6]

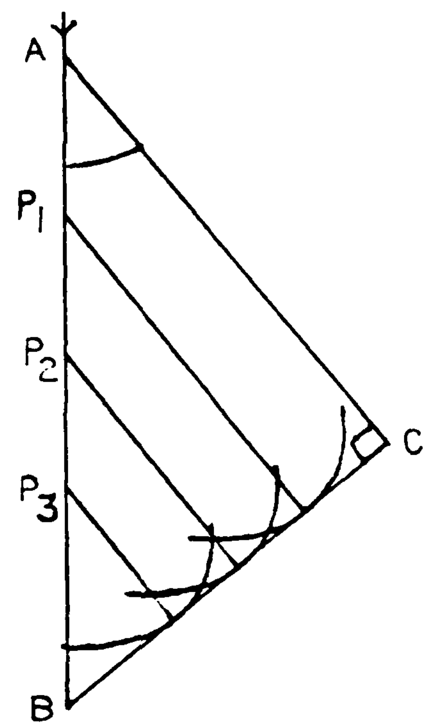

Figure 1. Huygens construction to illustrate coherence

Much of the research in Cerenkov radiation has been

limited to the optical regions, these being favored over the microwave region. The results from the optical radiation are expressed in terms of Fourier components for both the fields and the radiated power. [Ref.2: p. 3750]

Since all the electrons in an accelerator bunch radiate coherently, microwave radiation can be important. The time structure of the fields formed by elec on bunches that are radiated coherently was investigated by Professors Neighbours and Buskirk of the Naval Postgraduate School in their published paper of 1985. [Ref.2: p. 3750]

II. THEORY AND OBJECTIVES

A. MAGNETIC RADIATION FIELD

Neighbours and Buskirk proceeded by determining the potential from the moving charge distribution and then obtaining the B field (in cgs units) from the potential by

$$\vec{B} = \vec{\nabla} \times \vec{A} \qquad (1)$$

The charge density function ρ_v and the current density $j_v = \rho_v v/c_0$ (v, the velocity, is in the positive z direction) have been assumed and concentrated along the z-axis so that

$$\rho_v(\vec{r},t) = \rho(z,t)\delta(x)\delta(y) \qquad (2)$$

Since the charge is assumed to move with constant shape, the z and t dependence of the charge is

$$\rho(z,t) = \rho_0(z-vt) \qquad (3)$$

where ρ_0 and ρ are charge per unit length. [Ref.2: p. 3750]

The potential $\vec{A}$ is found to be

$$\vec{A}(\vec{r},t) = (\vec{v}/c_0) \int R^{-1} \rho(r',t')dz \qquad (4)$$

where $\vec{R} = \vec{r}-\vec{r}'$ and $t' = t - |r-r'|/c$ (the retarded time) and c is the speed of light in the medium. [Ref.2: p. 3750]

Equation (3) can be used in the potential equation and, defining a new variable $u(z') = z'-vt'$, with v defined as the particle velocity, $\vec{A}$ can be written as

$$\vec{A}(\vec{r},t) = (\vec{v}/co)\int R^{-1}\,f_0(u)dz \qquad (5)$$

The function $u(z')$ can be written as

$$u(z') = z'-vt+(v/c)[x^2+y^2+(z-z')^2]^{1/2} \qquad (6)$$

since the motion of the charge is confined to the z axis. [Ref.2: pp. 3750-3751]

Because $\vec{A}$ has only a z component, the B field, calculated from (1), has only x and y components; thus $B_x = \partial(A_z)/\partial y$ and $B_y = -\partial(A_z)/\partial x$. Considering the x component only,

$$B_x = (v/co)\int(\partial R^{-1}/\partial y)f_0(u)dz' + (v/co)\int R^{-1}(\partial f_0(u)/\partial y)dz' \quad (7)$$

At large distances, the first integral can be neglected since it will fall off as R^{-2}. Then the x-component of the B field can be written as

$$B_x = (v^2/cco)\int(y/R^2)\,f_0'(u)dz' \qquad (8)$$

where $\rho'_0(u)$ is the derivative with respect to u. Similarly, the y-component can be written as

$$B_y = (v^2/cc_0)\int(-x/R^2)\rho'_0(u)dz \qquad (9)$$

Combining these two components and using cylindrical coordinates, (s,Θ,z) where $s = (x^2+y^2)^{1/2}$, the magnitude of total magnetic field, B, is written as

$$B = (v^2/cc_0)\int(s/R^2)\rho'_0(u)dz \qquad (10)$$

and occurs in the direction of Θ, i.e. tangential. [Ref.2: p. 3751]

A similar derivation can be made in order to find the magnitude of the E field. It is also true that, in the Cerenkov case, $E/B = c/c_0$, which, for plane waves, is the usual relation between the electric and magnetic fields. [Ref.2: p. 3752]

B. TIME DEVELOPMENT

Considering the function $u(z')$, as described in equation (6), we can determine that the first two terms of the equation are a straight line in the u-z' plane and the last term is a hyperbola which opens in the positive u direction and has asymtotic slopes of $1 \pm (v/c)$. The straight line part of this function has a unit slope and a time dependent

intercept. The combination of these two curves results in the curve $u(z')$. Figure 2 [Ref.2: p. 3751] indicates what this curve would look like for the Cerenkov case with $v>c$. The time indicated in Figure 2 increases from t_1 to t_3. The curve will move downward with increasing time due to the negative second term of equation (6). [Ref.2: p. 3751]

The contribution to the B fields of equation (10) is due to changing currents (where ρ_0' is nonzero). A ramp front current pulse, for example, will have a derivative which is a constant square valued pulse whose magnitude is ρ_m'. This pulse is depicted in the right side of Figure 2. Only the positive pulse is considered. [Ref.2: p. 3751]

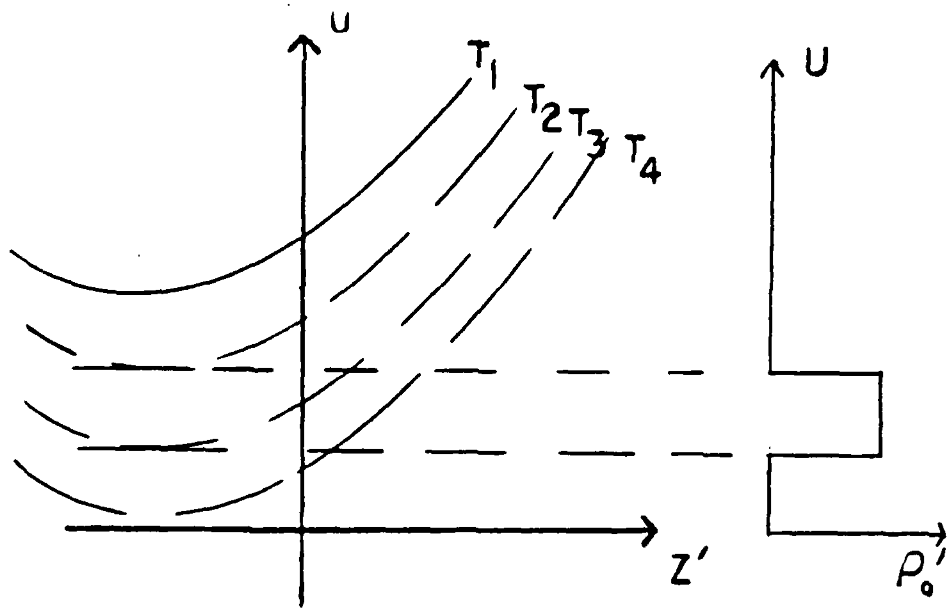

Figure 2. Function u = z-vt

For this example, the function $u(z')$ will be above the nonzero portion of ρ_0' for large negative times, and for

small positive times. During these periods, ρ_0' will be zero and therefore, the B field will be zero. When $u(z')$ becomes tangent to the upper part of the ρ_0' pulse, namely u_1, then there is a nonzero contribution made by ρ_0' to the B field and it becomes nonzero. The magnitude of the B field will continue to increase until $u(z')$ is tangent to the lower part of ρ_0', called u_2 in Figure 2. At later times the integral splits into two parts, and since ρ_0' is constant, the B field will decrease. This is due to the fact that the u function is turned upward and the area under the curve will decrease. [Ref.2: p. 3751]

C. OBJECTIVES

The objective of this thesis is to solve for the magnitude of the B field over a finite path. In order to do this, the limits of integration for equation (10) must be found and a computer program written to solve the integral and graph the magnitude of the B field, for various situations. For this calculation, time begins at zero, when the beam is fired.

III. EQUATION DEVELOPMENT

The derivation of equations in this chapter is based upon unpublished and untitled notes by Professor J.R. Neighbours.

A. CALCULATING THE B FIELD

Equation (10) can be written with finite limits of integration as

$$B = (v^2/cc_0)\int_{z'_i}^{z'_f}(sR^{-2})\,\rho'_0(u)dz \qquad (11)$$

If $v^2/cc_0 = n\beta^2$ and $\rho'_0(u) = \rho'_m$ = constant, then equation (11) becomes

$$B = n\beta^2 s\rho'_m\int_{z'_i}^{z'_f}R^{-2}dz \qquad (12)$$

where $s = (x^2+y^2)^{1/2}$ and $R^2 = s^2 + (z-z')^2$ or $R^2 = s^2+w^2$, where $w = z-z'$. Substituting the variable w into equation (12) and integrating with respect to w, the solution becomes

$$B = n\beta^2\rho'_m[\tan^{-1}(w_1/s)-\tan^{-1}(w_2/s) \qquad (13)$$

where $w_1 = z-z'_i$ and $w_2 = z-z'_f$. Thus, the problem is to find the values of w_1 and w_2.

B. CALCULATING THE LIMITS OF INTEGRATION

1. Situations Encountered For The Finite Path

There are three basic situations encountered in this study of the B field and each depends upon the position of the observer in relation to the Cerenkov angle, θ_c. Figures 3, 4, and 5 illustrate the three different situations. In each of these figures, the beam length is L, and the point, P(z,s), is the position of the observer.

The three situations can be related to the position of the minimum of the function $u(z')$, i.e., the path can be to the right, left, or centered about the minimum. If $v/c=\beta'$, and substituting the value of s, equation (6) can be written as

$$u(z') = z' - vt - \beta'[s^2+(z-z')^2]^{1/2} \qquad (14)$$

This function has a minimum at $\tan\theta_c = \pm s/(z-z')$; therefore, the minimum occurs on the Cerenkov cone when $z-z'$ is such that $\theta = \theta_c$.

The criterion for the path to be to the right is that θ_1 in Figure 3 must be greater than θ_c; for the path to be to the left, θ_2 in Figure 4 must be less than θ_c; for the path to be centered about the minimum, θ_1 must be less than θ_c and θ_2 must be greater than or equal to θ_c, as shown in Figure 5.

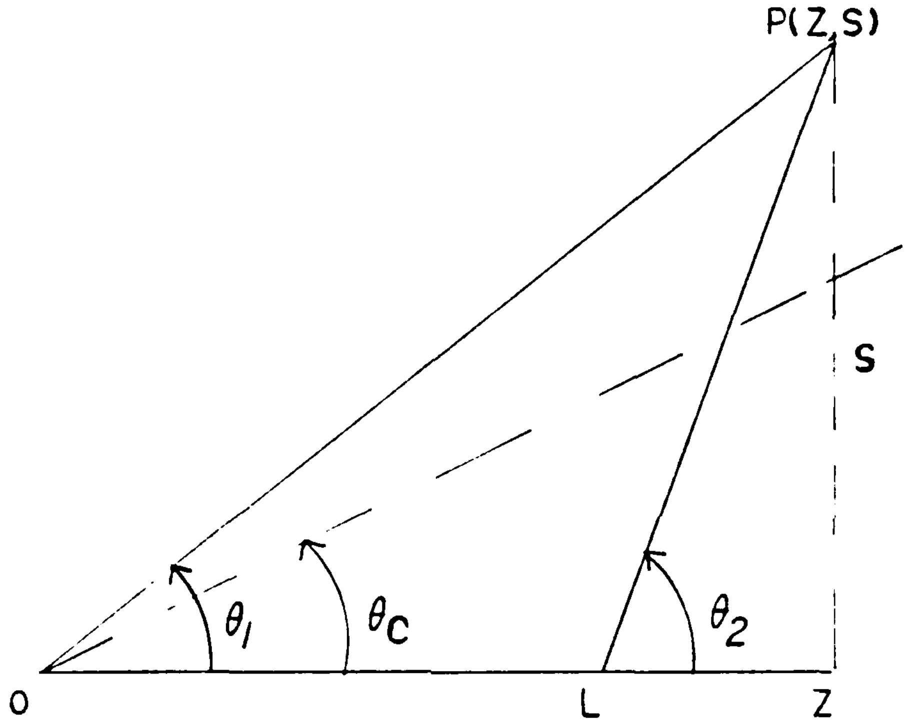

Figure 3. Path To The Right

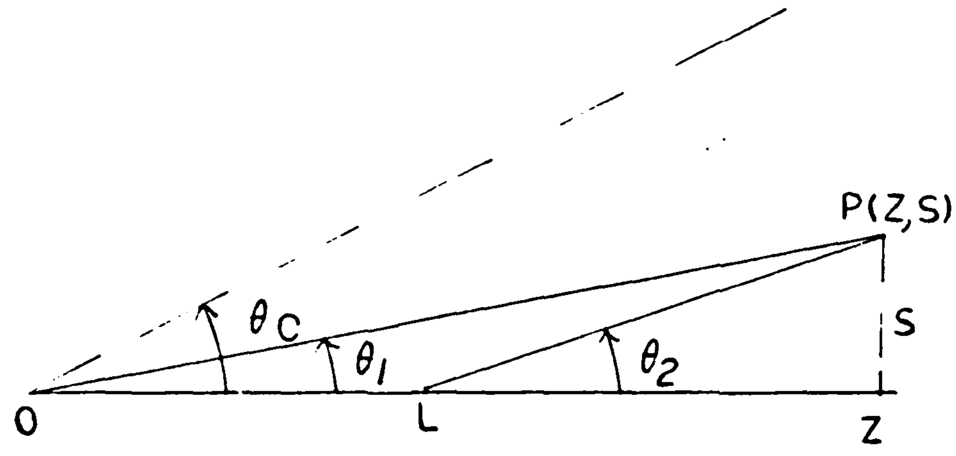

Figure 4. Path To The Left

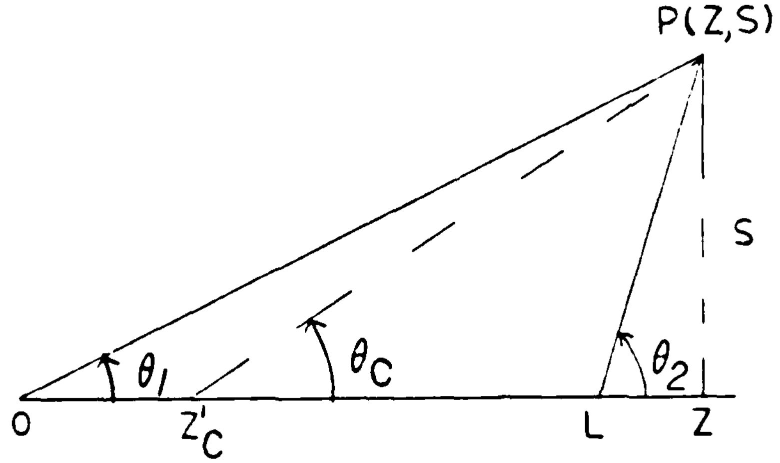

Figure 5. Path Centered About The Minimum

The rectangle in the u-z′ plane (Figure 6) is formed by the path length, L, and the limits on the ramp function, u_1 and u_2; the corners are labeled ABCD.

a. Path To The Right

The relationship between the path and the minimum of u(z′) is shown in Figure 6. The B field will be encountered first at time T_A and will go to zero again at time T_D. The limits of integration for the curve, as it passes through the rectangle bounded by T_A, T_B, T_C, and T_D, are the points of intersection of the curve and the rectangle.

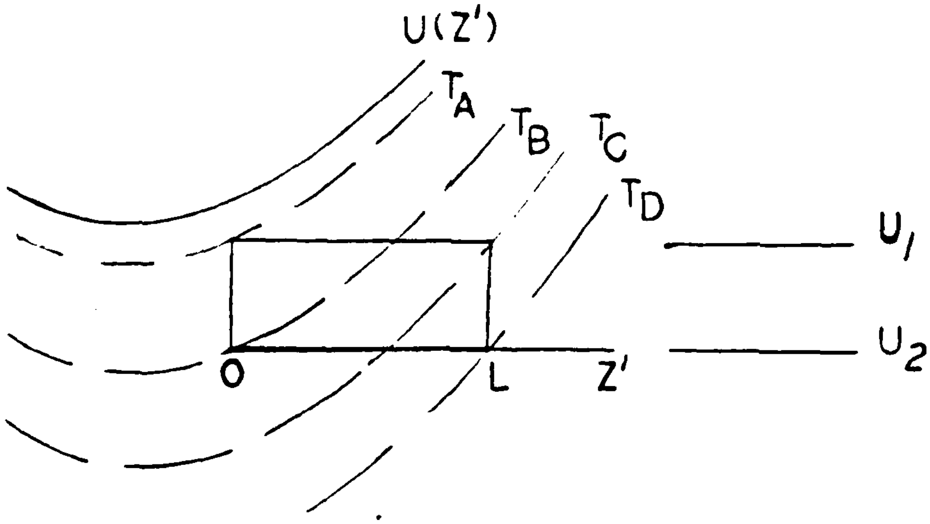

Figure 6. Relation of u(z′) to Path to the Right

For the path to the right, as well as the other two cases, the values of these boundary times are found by solving equation (14), having substituted the appropriate values of z′ and u(z′). The results are

$$T_A = [\beta'(s^2+z^2)^{1/2} - u_1]/v \qquad (15)$$

$$T_B = [\beta'(s^2+z^2)^{1/2} - u_2]/v \qquad (16)$$

$$T_C = [L + \beta'(s^2+(z-L)^2)^{1/2} - u_1]/v \qquad (17)$$

$$T_D = [L + \beta'(s^2+(z-L)^2)^{1/2} - u_2]/v \qquad (18)$$

The case illustrated in Figure 6 is one in which T_C is greater than T_B. The condition for this case to occur is that $u_1 - u_2 < L + \beta'[(s^2+(z-L)^2)^{1/2} - (s^2+z^2)^{1/2}]$. There are two other cases, namely, when T_C is less than T_B and T_C is equal to T_B. The derivation of the equations for the limits of integration for the first case will be described; the equations for the last two cases are found in a similar manner.

Suppose $T_A<T<T_B$ and $u(z)$ is positioned at time T as illustrated in Figure 7a. The lower limit of integration for equation (12), z'_i, is zero in this case and

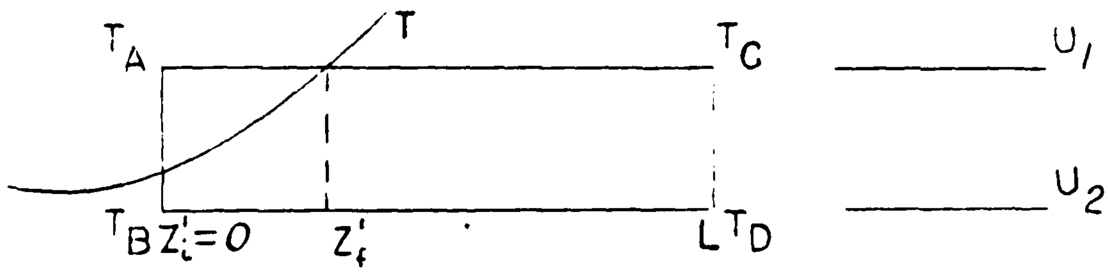

Figure 7a. $T_C>T_B$: $T_A<T<T_B$

z'_f is found by solving equation (14). If $z'=z'_f$, $u(z')=u_1$, and a new variable, $A_1 = u_1+vt$, is introduced, the solution of this quadratic equation becomes

$$z_f' = \{(\beta'^2 z - A_1) + \beta'[(z-A_1)^2 - s^2(\beta'^2-1)]^{1/2}\}/(\beta'^2-1) \qquad (19)$$

Only the positive solution for the quadratic equation is valid because of the position of the minimum for the path to the right.

The last two situations for the $T_C > T_B$ case are $T_B < T < T_C$ and $T_C < T < T_D$, which are illustrated in Figures 7b and 7c, respectively. For these last two situations, a new variable, A_2, is used and defined as $u_2 + vt$. After solving equation (14) for the lower and upper integral limits, we find that for $T_B < T < T_C$

$$z_i' = \{(\beta'^2 z - A_2) + \beta'[(z-A_2)^2 - s^2(\beta'^2-1)]^{1/2}\}/(\beta'^2-1) \qquad (20)$$

and z_f' is calculated by using equation (19). For $T_C < T < T_D$, z_i' is found by using equation (20) and $z_f' = L$.

As mentioned previously, there are two more cases for the path to the right, where $T_C < T_B$ and $T_C = T_B$. For the case of $T_C < T_B$, the condition is that

$$u_1 - u_2 > L + \beta'[(s^2+(z-L)^2)^{1/2} - (s^2+z^2)^{1/2}]$$

and for $T_C = T_B$

$$u_1 - u_2 = L + \beta'[(s^2+(z-L)^2)^{1/2} - (s^2+z^2)^{1/2}]$$

Figures 8 and 9 illustrate the last two cases for the path to the right.

The limits of integration for these last cases are found in the same way as for the first case. A summary

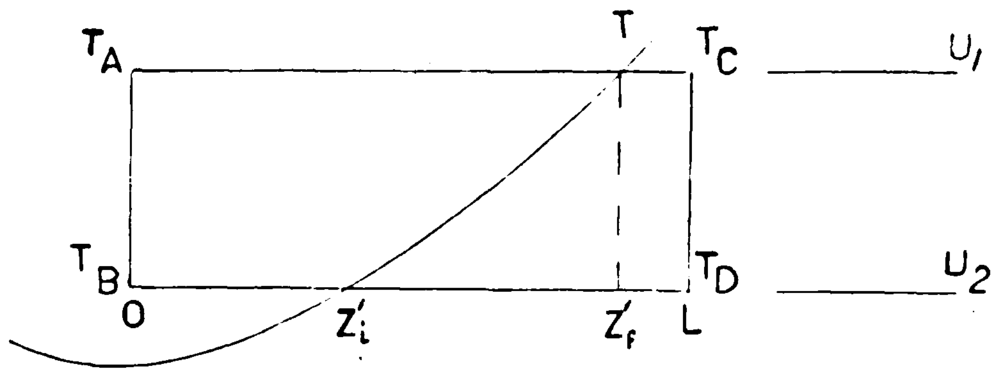

Figure 7b. $T_C > T_B$: $T_B < T < T_C$

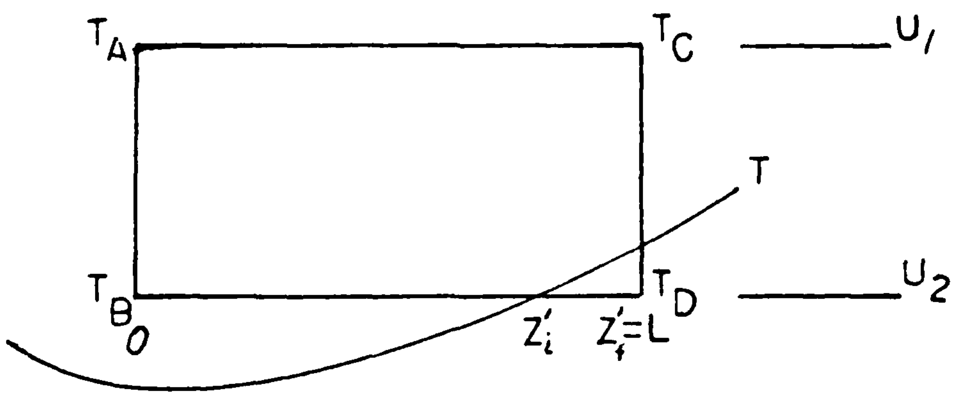

Figure 7c. $T_C > T_B$: $T_C < T < T_D$

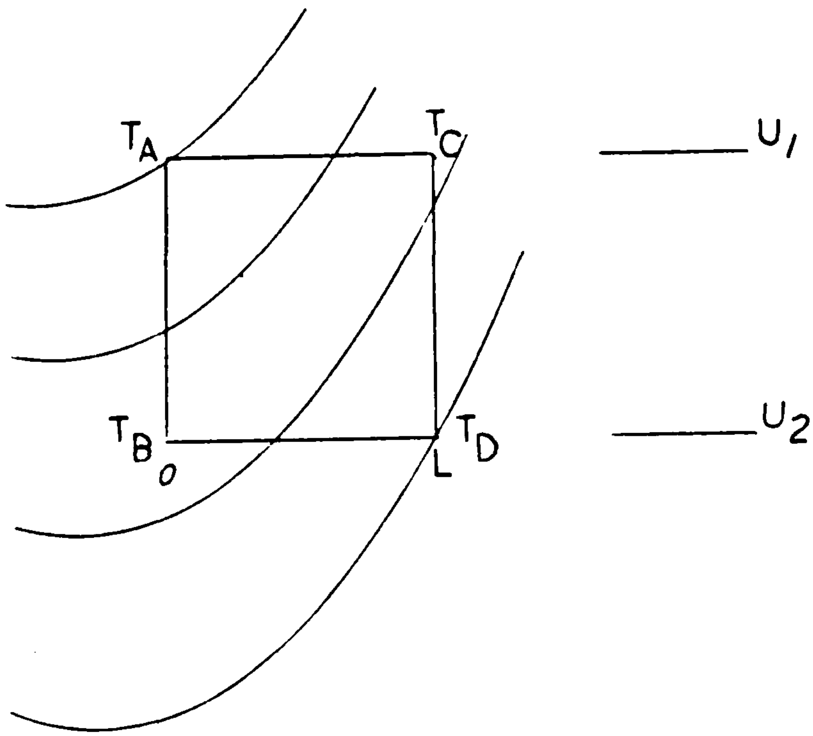

Figure 8. Path To The Right: $T_C < T_B$

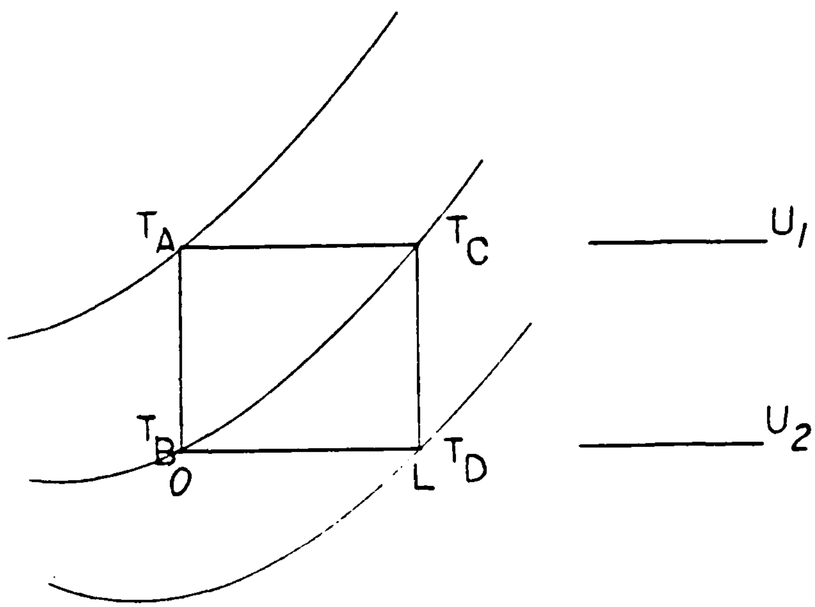

Figure 9. Path To The Right: $T_C = T_B$

of the limits of integration for the path to the right is listed in Table 1, where

$$a = \{(\beta'^2 - A_2) + \beta'[(z - A_2)^2 - s^2(\beta'^2 - 1)]^{1/2}\}/(\beta'^2 - 1)$$

and

$$b = \{(\beta'^2 z - A_2) + \beta'[(z - A_2)^2 - s^2(\beta'^2 - 1)]^{1/2}\}/(\beta'^2 - 1).$$

TABLE 1

LIMITS OF INTEGRATION: PATH TO THE RIGHT

$T_C > T_B$:	$T_A < T < T_B$	$T_B < T < T_C$	$T_C < T < T_D$
z'_i	0	b	b
z'_f	a	a	L
$T_C < T_B$:	$T_A < T < T_C$	$T_C < T < T_B$	$T_B < T < T_D$
z'_i	0	0	b
z'_f	a	L	L
$T_B = T_C$:	$T_A < T < T_B$	$T_B < T < T_D$	
z'_i	0	b	
z'_f	a	L	

b. Path To The Left

The relationship between the minimum of $u(z)$ and the path is shown in Figure 10.

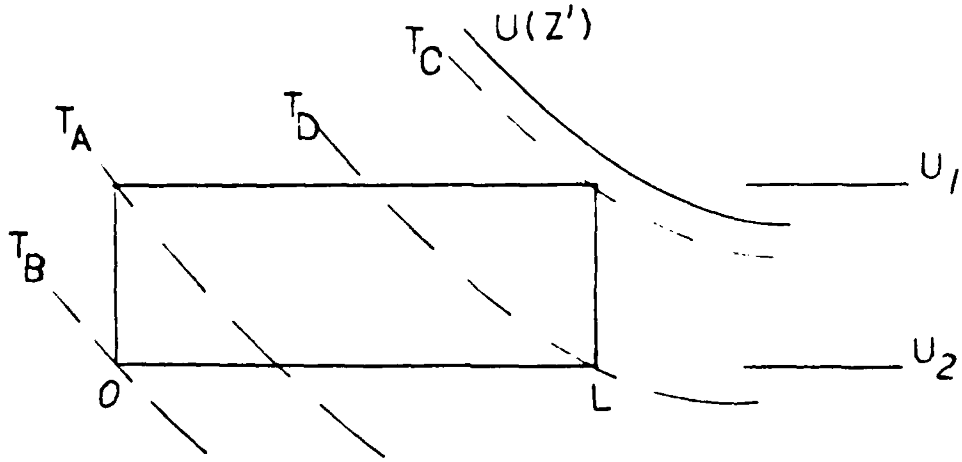

Figure 10. Relation of $u(z')$ to Path to the Left

The limits of integration for the path to the left are found in the same manner as in the path to the right. However, due to the position of the minimum with respect to the path, only the negative part of the quadratic solution will be used. The three cases for the path to the left are summarized in Table 2; the conditions for each are included.

TABLE 2

CASES AND CONDITIONS FOR THE PATH TO THE LEFT

Cases	Conditions
$T_A > T_D$	$u_1 - u_2 < \beta'[(s^2+z^2)^{1/2} - (s^2+(z-L)^2)^{1/2}] - L$
$T_A < T_D$	$u_1 - u_2 > \beta'[(s^2+z^2)^{1/2} - (s^2+(z-L)^2)^{1/2}] - L$
$T_A = T_D$	$u_1 - u_2 = \beta'[(s^2+z^2)^{1/2} - (s^2+(z-L)^2)^{1/2}] - L$

These cases are shown in Figures 11a, b, and c; the limits of integration are listed in Table 3 with

$$aa = \{(\beta'^2 z - A_1) - \beta'[(z-A_1)^2 - s^2(\beta'^2-1)]\}/(\beta'^2-1)$$

and

$$bb = \{(\beta'^2 z - A_2) - \beta'[(z-A_2)^2 - s^2(\beta'^2-1)]\}/(\beta'^2-1)$$

TABLE 3

LIMITS OF INTEGRATION: PATH TO THE LEFT

$T_A < T_D$:	$T_C < T < T_A$	$T_A < T < T_D$	$T_D < T < T_B$
z'_i	aa	0	0
z'_f	L	L	bb
$T_A > T_D$:	$T_C < T < T_D$	$T_D < T < T_A$	$T_A < T < T_B$
z'_i	aa	aa	0
z'_f	L	bb	bb
$T_A = T_D$:	$T_C < T < T_A$	$T_D < T < T_B$	
z'_i	aa	0	
z'_f	L	bb	

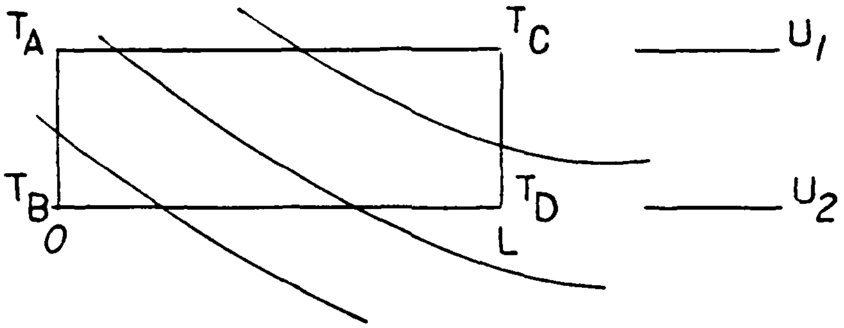

Figure 11a. Path To The Left: $T_A > T_D$

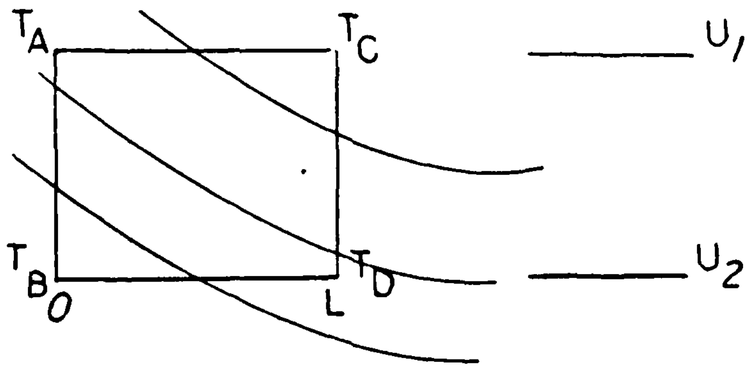

Figure 11b. Path To The Left: $T_A < T_D$

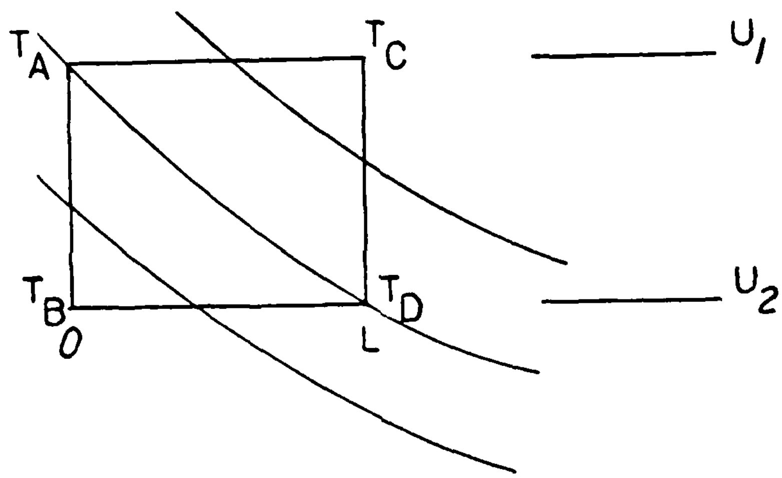

Figure 11c. Path To The Left: $T_A = T_D$

c. Centered About The Minimum

This case is slightly different from the first two, as can be seen in Figure 12. The minimum occurs between 0 and L at z_c', so that as shown in Figure 5, the position of the observer makes the Cerenkov angle with respect to the direction of the beam. For this case, new

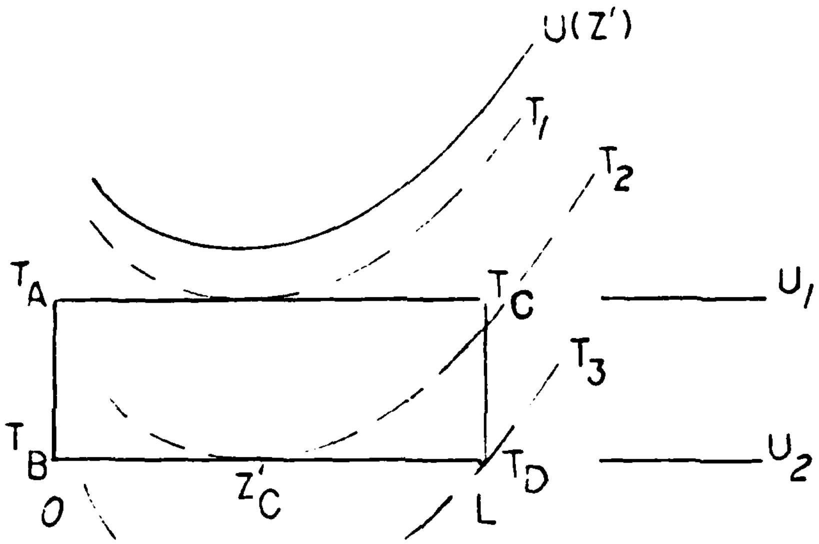

Figure 12. Centered About the Minimum

times must be introduced: T_1, when the minimum just contacts the u_1 line, T_2, when the minimum contacts the u_2 line and T_3, the final time. Calculating the times from equation (14), we find that the results are

$$T_1 = \{z_c' + \beta'[s^2 + (z-z_c')^2]^{1/2} - u_1\}/v$$

$$T_2 = \{z_c' + \beta'[s^2 + (z-z_c')^2]^{1/2} - u_2\}/v$$

and T_3 will be the larger of the T_B or T_D, as previously defined in equations (16) and (18), respectively.

Considering the situation where $T_1 < T < T_2$, as shown in Figure 13, it can be seen that both solutions to the quadratic equation may be utilized, such that

$$z'_+ = \{(\beta'^2 z - A_1) + \beta'[(z-A_1)^2 - s^2(\beta'^2-1)]^{1/2}\}/(\beta'^2-1) \qquad (21)$$

and

$$z'_- = \{(\beta'^2 z - A_1) - \beta'[(z-A_1)^2 - s^2(\beta'^2-1)]^{1/2}\}/(\beta'^2-1) \qquad (22)$$

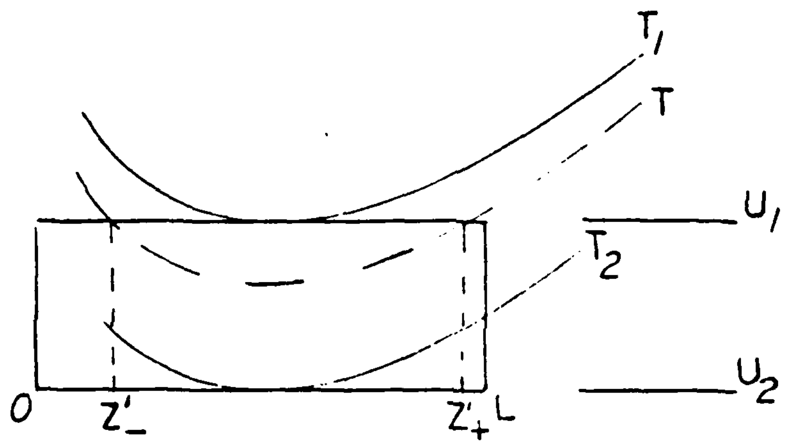

Figure 13. $T_1 < T < T_2$

With these two solutions, the following conditions, listed in Table 4, are imposed in order to choose the proper limits of integration.

TABLE 4

CONDITIONS FOR THE LIMITS OF INTEGRATION: $T_1 < T < T_2$

Condition	z'_i	z'_f
$z'_- \leq 0$	0	
$z'_- > 0$	z'_-	
$z'_+ \geq L$		L
$z'_+ < L$		z'_+

For the last case, $T_2 < T < T_3$, there are two integrals to solve, as shown in Figure 14.

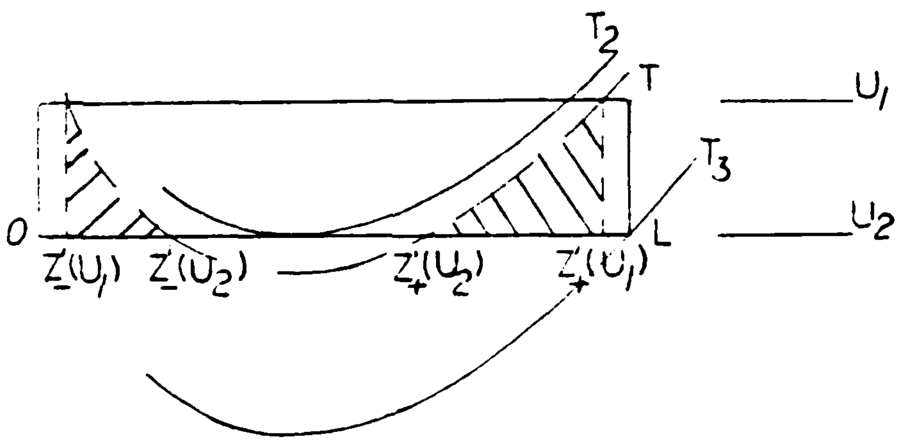

Figure 14. $T_2 < T < T_3$

For the first integral, $z'_-(u_1)$ is found by using equation (22) and

$$z'_+(u_2) = \{\beta'^2 z - A_2) - \beta'[(z-A_1)^2 - s^2(\beta'^2 - 1)]^{1/2}\}/(\beta'^2 - 1) \qquad (23)$$

In this case z'_f will always be $z'_-(u_2)$. However, z'_i will equal $z'_-(u_1)$ when the latter value is greater than zero; otherwise, z'_i will equal zero.

Similarly, the limits for the second integral, $z'_+(u_1)$ and $z'_+(u_2)$ will be the corresponding solutions to the above equations in which the second term is positive. In this case, z'_i will always be $z'_+(u_2)$, whereas z'_f will equal $z'_+(u_1)$ if the latter is less than L, otherwise z'_f will equal L.

The total B field will be the sum of these two integrals.

Table 5 lists a summary of the limits of integration for the path centered about the minimum.

TABLE 5

LIMITS OF INTEGRATION: PATH CENTERED ABOUT THE MINIMUM

	$z'_- \leq 0$	$z'_- > 0$	$z'_+ \geq L$	$z'_+ < L$
$T_1 < T < T_2$				
z'_i	0	z'_-		
z'_f			L	z'_+
$T_2 < T < T_3$				
FIRST INTEGRAL:				
z'_i	0	z'_-		
$z'_f = z'_-(u_2)$				
SECOND INTEGRAL:				
$z'_i = z'_+(u_2)$				
z'_f			L	$z'_+(u_1)$

C. SUMMARY

In each of the above situations, if the values for z_i and z_f are substituted into the equations for w_1 and w_2, respectively, the limits of integration can be calc .ated and used to solve equation (13), the magnitude of the B field.

IV. CALCULATIONS AND ANALYSIS

A. CALCULATIONS

Having derived the formaulas for the limits of integration, the next step was to write a computer program to calculate the B fields and graph it against time.

The FORTRAN program is interactive and has a variable input for the values of u_1, u_2, β, n, ρ_m', s, z and L. The values for the first five quantities were chosed to be: u_1=100 cm, u_2=50 cm, β=.99, n=1.111111 and ρ_m'=1. Various values for s, z and L were used.

Based on the input, this program will choose what type of situation is occurring, whether right, left or center. It will calculate the B field during the time the $u(z')$ curve transits the rectangle in the u-z' plane, and will graph B vs time(nsec).

The graphics part of this program is based on a code written by Professor J.R. Neighbours for use on a Textronix computer; the main part of the program is an original work.

Calculations were carried out for various beam lengths, using different values for s; numerous values of z were used and the corresponding B field graphs were obtained. After studying these curves, a beam length of 1500 was chosen with s values of 1500 and 3000. Graphs for selected

values of z were compared; these graphs are shown in Figures 20 through 42, found in Appendix A.

B. MINIMUM TIME

In analyzing the three situations, the minimum time taken for the radiation to reach the observer was determined. Figure 15 shows the situation which will be used to find the time in each of the three cases.

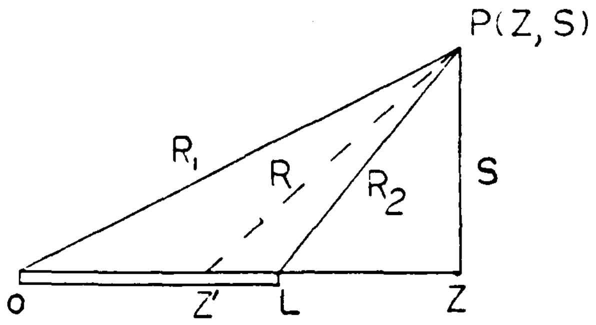

Figure 15. Path of Beam and Radiation (z and R)

The beam emerges at 0 and travels to L at constant velocity v, where $v = \beta c_0$. Radiation is emitted when the head of the beam is at z'. The radiation then travels at a constant velocity, c, to the observer at P.

The time it will take the radiation to reach the observer is given by

$$t(z') = z'/(\beta c_0) + (nR)/c \qquad (24)$$

Since $R^2 = (z-z')^2$, equation 24 can be written as

$$t(z') = z'/\beta c_0) + n/c_0)[(z-z')^2 + s^2]^{1/2} \quad (24a)$$

As can be seen in Figure 16, there is a minimum time for the path centered about the minimum. It occurs at the point z'_c (at the Cerenkov angle, θ_c. The values used in this case are z=4000, L=1500 and s=1500. This graph verifies the following calculation for the minimum time occuring at the Cerenkov angle.

$$\begin{aligned} dt/dz' &= 1/\beta c_0 + (1/2)(n/c_0)[(z-z')^2 + s^2]^{-1/2} 2(z-z') \\ &= 1/\beta c_0 + (n/c_0)[(z-z')/R] \\ &= 1/\beta c_0 + (n/c_0)\cos\theta = 0 \end{aligned}$$

This equation will equal zero when the value of $\cos\theta$ is $1/n\beta$; this implies that $\theta = \theta_c$.

Figures 17 and 18 show that there is not minimum time over the length of the beam, L=1500, for the paths to the right and left.

Although this analysis confirms that the minimum occurs at the Cerenkov angle, there is no correlation between the time in Figures 17, 18 and 19, and the time in the B field radiation graphs. The problem stems from the fact that T_A through T_D depend on the values of u_1 and u_2, and T_C and T_D also depend on L, while equation (24) depends on neither of these quantities.

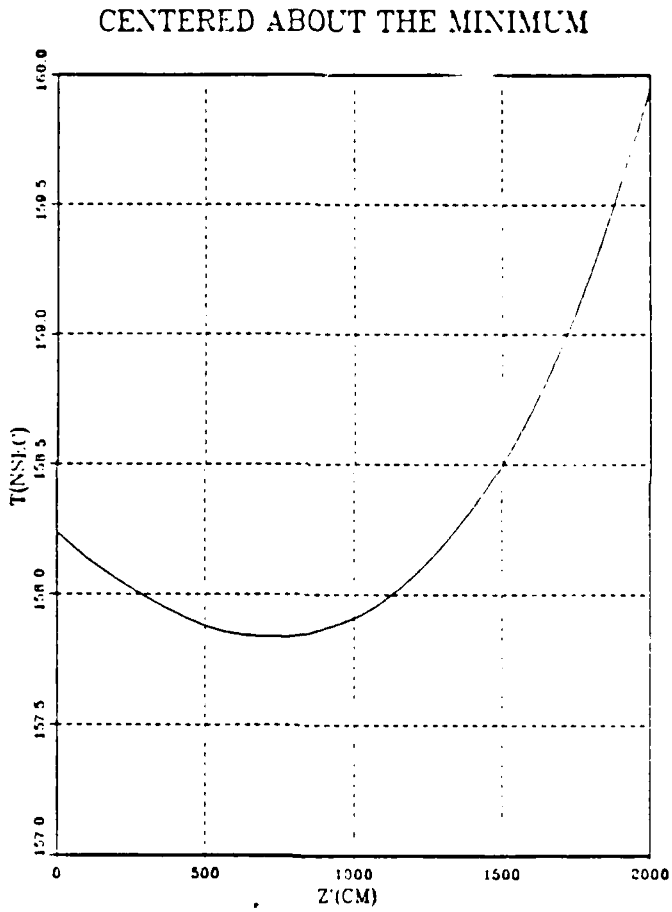

Figure 16: Centered About the Minimum

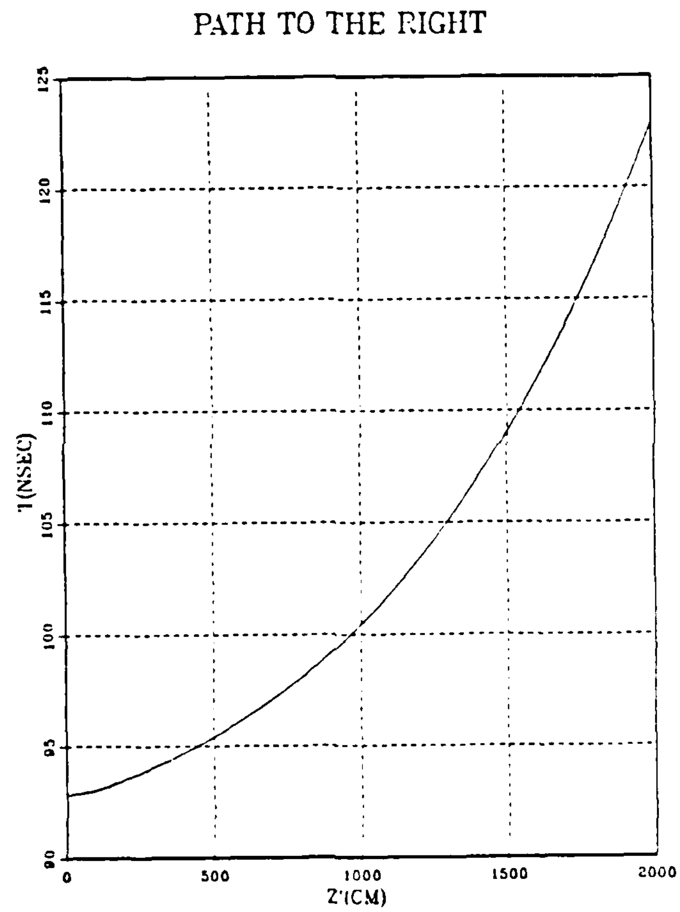

Figure 17: Path to the Right: No Minimum Time

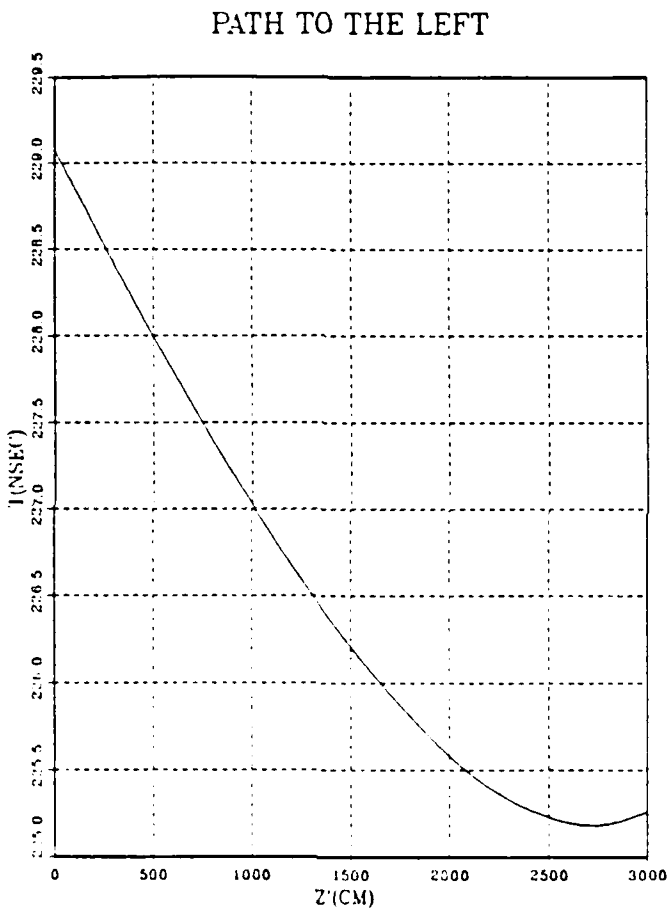

Figure 18: Path to the Left: No Minimum Time

C. ANALYSIS OF THE B FIELD GRAPHS

In analyizing the B field graphs, it was decided to look for similar characteristics and shapes. In this analysis two cases were considered, each with L=1500; the comparison was made between the graphs for s=3000 and s=1500.

Figure 19 is a graph of s/L vs z/L. This graph indicates the boundary regions for time, i.e., line #1 is $T_C = T_B$, and line #2 is $T_A = T_D$; these values are based on a Δu of 50 cm and the ratio $\Delta u/L = .03333$, where $\Delta u = u_1 - u_2$. The time region to the left of line #1 is $T_C > T_B$, and the region to the right of line #2 is $T_A > T_D$. The region between line #1 and #2 contains the times $T_C < T_B$ and $T_A < T_D$. The graph also indicates the Cerenkov region, the area between the dashed lines. The regions labeled RIGHT, CENTER and LEFT correspond to the position of the observer as previously described. The boundary lines between these regions are the dashed lines. Each of the B fields graphs can be placed in different time regions as indicated in Figure 19. Figures 20 through 28 are all graphs of the path to the right for which $T_C > T_B$; these graphs lie to the left of line #1 and are indicated by the symbol x in Figure 19. Figures 20 through 26 are for s=1500, while Figures 27 and 28 are for s=3000. Comparing these graphs, it can be seen that there is a similarity in shape; as the z value gets closer to the Cerenkov region, for each s case, the initial peak

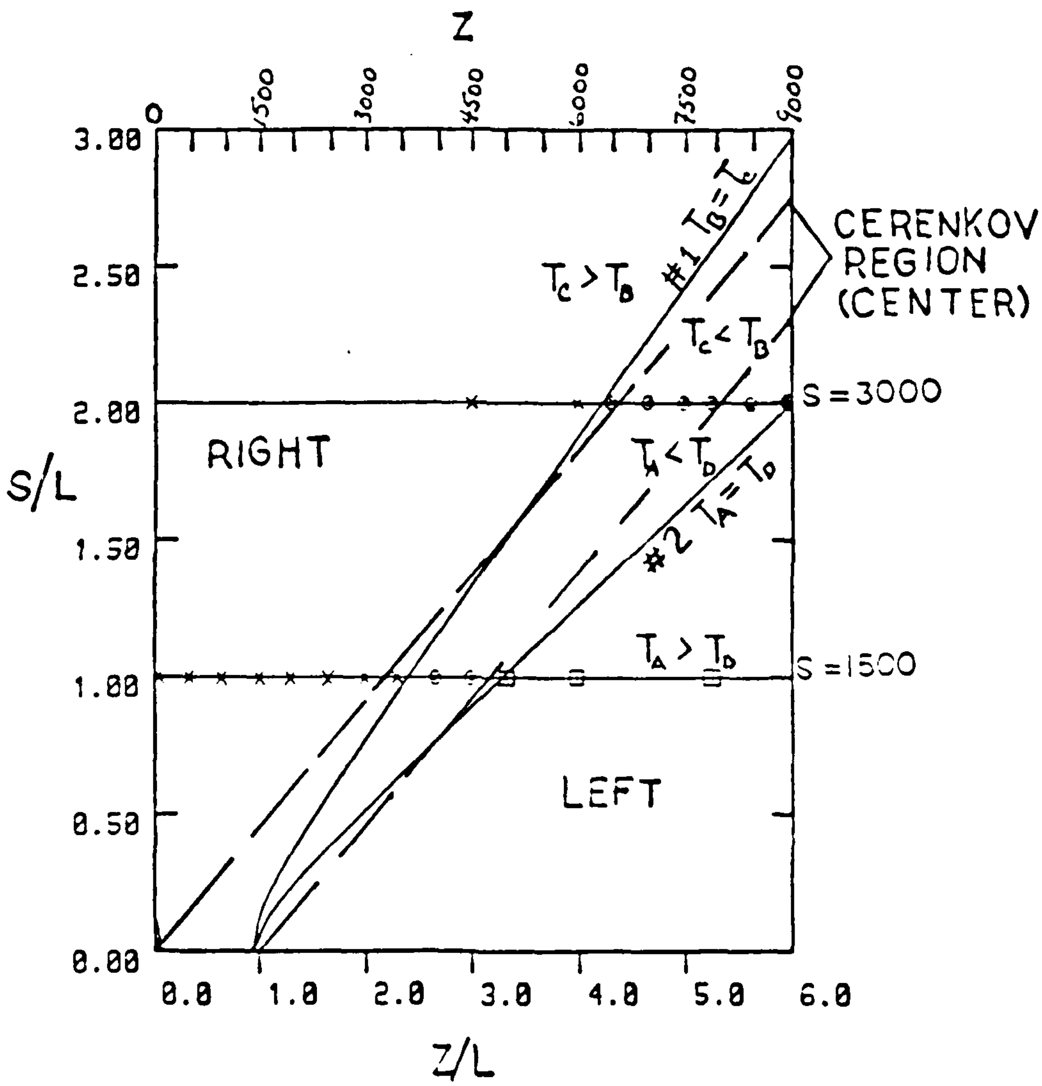

Figure 19: Graph of z/L vs s/L

increases in magnitude. This is expected, since the radiation should be greatest in the Cerenkov region. The duration of the pulse decreases as z gets farther from the source (L=0); also, it is first seen at a later time.

Figures 29 through 34 (29-31: s=1500; 32-34: s=3000) show the B field in the Cerenkov region. The characteristics of the curves shown in Figures 30 through 34 are such that the field increases, levels off and decreases; there are no distinctive peaks. However, Figure 29 shows characteristics of the path to the right, where $T_C > T_B$, and z is close to the Cerenkov region. Although this curve falls into the Cerenkov region, it is also in the time region for $T_C > T_B$, to the left of line #1 and is indicated by the symbol x in Figure 19. Its shape is dependent on the relationship between T_C and T_B. The other graphs in the Cerenkov region fall in the time regions $T_C < T_B$ and $T_A < T_D$, between lines #1 and #2. These are indicated by the symbol ○ in Figure 19. Other examples of the shape being dependent on the time region are shown in Figures 35 and 36, which indicate a B field for the path to the right and path to the left, respectively. The shape of these curves is very similar to that of the graphs in the Cerenkov region between lines #1 and #2. The field in Figure 35 falls into the time region $T_C < T_B$ and the field in Figure 36 falls into the time region $T_A < T_D$. Both of these cases are indicated by the symbol ○ in Figure 19, since they

fall between line #1 and #2. Thus it would seem that the placement of each case in relation to the time boundaries is very important in determining the shape of the B field curve.

Figure 37 (path to the left) shows a field which is extremely close to the time boundary $T_A = T_D$. Because this is almost on the boundary, the flat part of the curve is just coming to a point. The other graphs for the path to the left (Figures 38 through 42) show characteristics similar to those of the path to the right. For these graphs, there is an initial peak and then the field falls off; again the magnitude is greater closer to the Cerenkov region. The first time the field is seen increases as z increases; however, unlike the path to the right, the duration of the field increases slightly as z increases. This increase in duration would be expected since, in the path to the left, the beam is coming toward the observer and not traveling away. Figures 38 through 42 all fall to the right of line #2, and are indicated by the symbol □ in Figure 19.

The curves in Figures 20 through 29 all fall in the time region $T_C > T_B$. There are four distinct points in these curves: the initial and final points, with two intermediate points. In each of these cases, the points correspond to T_A, T_B, T_C and T_D, in that order. This indicates that the initial rapid increase in the field is

due to the u function traveling through the distance Δu. This same thing occurs in Figures 38 through 42, in which the time region is $T_A > T_D$. However, these points correspond to T_C, T_D, T_A and T_B, the case for the path to the left.

Figures 30 through 33, show B fields for cases which fall well within the Cerenkov region. In each of these cases, there are six distinct points: the initial and final points, with four intermediate points. In Figure 30, for example, these points correspond to T_1, T_A, T_C, T_2, T_B and $T_3 = T_D$. Figure 34 shows only four distinct points, corresponding to T_C, T_A, T_D and T_B. This case is almost on the boundary for the Cerenkov region; it shows the four points corresponding to the path to the left, with $T_A < T_D$, rather than the six points for the center case.

V. CONCLUSIONS AND RECOMMENDATIONS

A. CONCLUSIONS

From this preliminary study, it would seem that the shape of the B field is determined by its placement within a time region, rather than exclusively by the position of the minimum, i.e., path to the right, left or centered about the minimum. In Figure 19, the boundary line #1 and #2 are the cutoffs for determining the characteristic shapes of the B field graphs. Between these two lines, the graphs show a period during which the radiation levels off. On either side of these lines, there is a radiation peak and the field falls off to a secondary peak and then continues to zero. When the study was undertaken, it was expected that the cutoff for characteristic shapes would be the position of the observer in relation to the Cerenkov region. Since the ime regions play such an important role, it would be simpler to study the radiation fields from graphs similar to that in Figure 19.

The maximum value of the B field, for a given s and L, is found to be in the path centered about the minimum, i.e., in the Cerenkov region.

The duration of the pulse decreases throughout the path to the right and well into the Cerenkov region. This is due to the fact that the beam is traveling away from the observer. For situations occurring close to the boundary

of the Cerenkov region and the path to the left, and continuing into the region for the path to the left, the duration of the pulse increases slightly. For these cases, the beam is traveling toward the observer.

In each case studied, as z increases, i.e., as the observer gets farther from the source, the pulse first appears at a later time.

It is difficult to predict the characteristics of a curve whose z value falls on or close to a boundary line (Figure 19), whether that be a time or path boundary. These characteristics include shape, flat topped or peaked, and the number of distinct points on the curve.

In analyzing graphs for different values of $\Delta u/L$, it was determined that as $\Delta u/L$ gets very small, i.e., equals 0.0001, all the time lines coincide. This would mean that all the graphs would have a peaked shape and the flat top curves would disappear, since there would be no region between the time line boundaries.

B. RECOMMENDATIONS

Since the shape of the B field curve is so closely related to the time regions in Figure 19, it is recommended that several other values of Δu be used for analysis, along with different values for s, the vertical coordinate of the observer's position, P(z,s), in the z-s plane, and for L, the beam length.

It is also recommended that some universal time scale be found to use in graphing the radiation fields. For this study, each graph begins at a different time, the time the u curve begins to transit the rectangle in the u-z plane. If each graph indicates the same time scale, it would be easier to conduct an analysis and comparison of the radiation fields.

Since there was a problem in correlating the minimum time with the B field graphs, it is recommended that further study be conducted in this area

In order to make it easier to study the graphs for the case centered about the minimum, it is recommended that the program Fields (Appendix B) be changed so that the print out of the graphs indicate the relationship between T_A and T_D, and T_B and T_C. Also, a listing of all the appropriate boundary times in each case would be valuable.

APPENDIX A

FIGURES: B FIELD CURVES

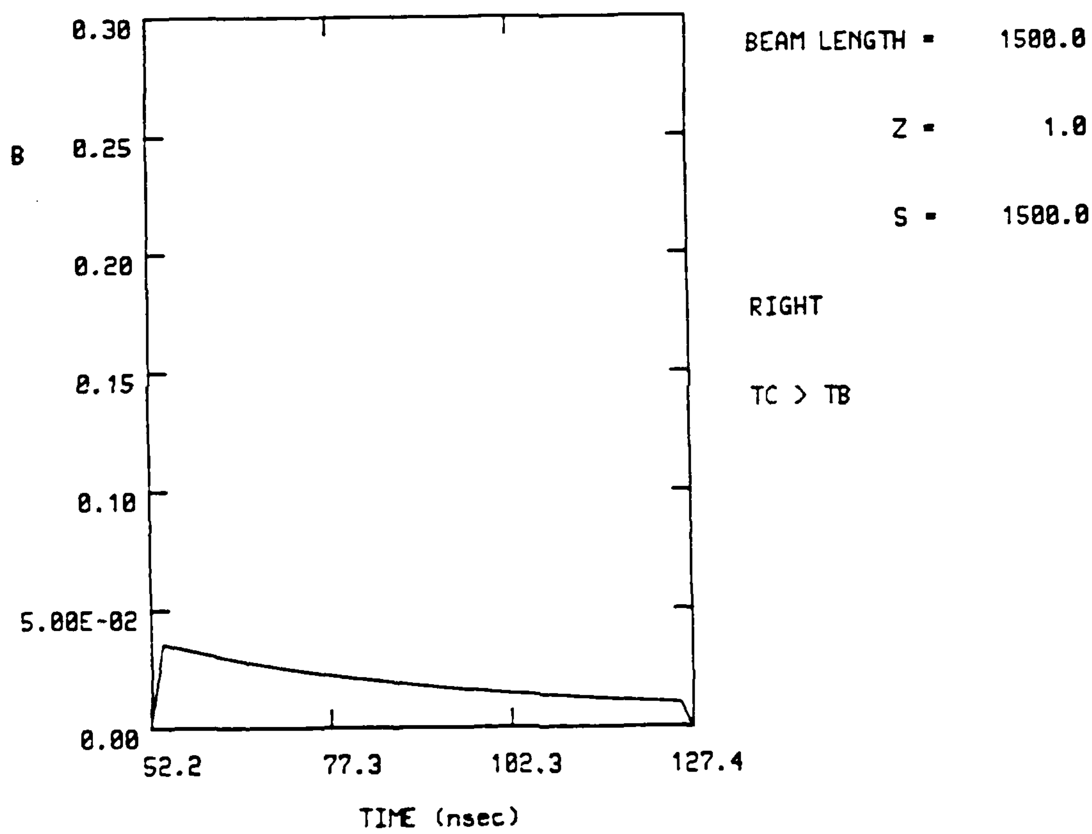

Figure 20: s=1500, z=1; Tc >Tb

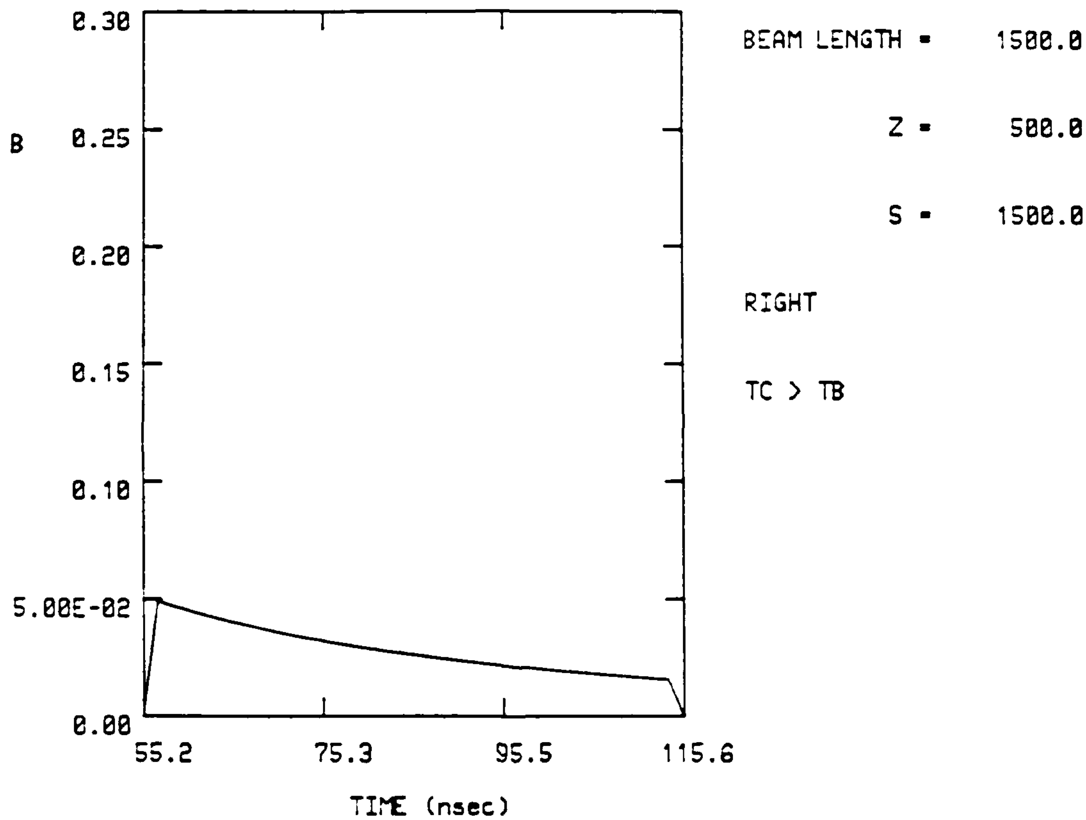

Figure 21: s=1500, z=500; Tc > T_B

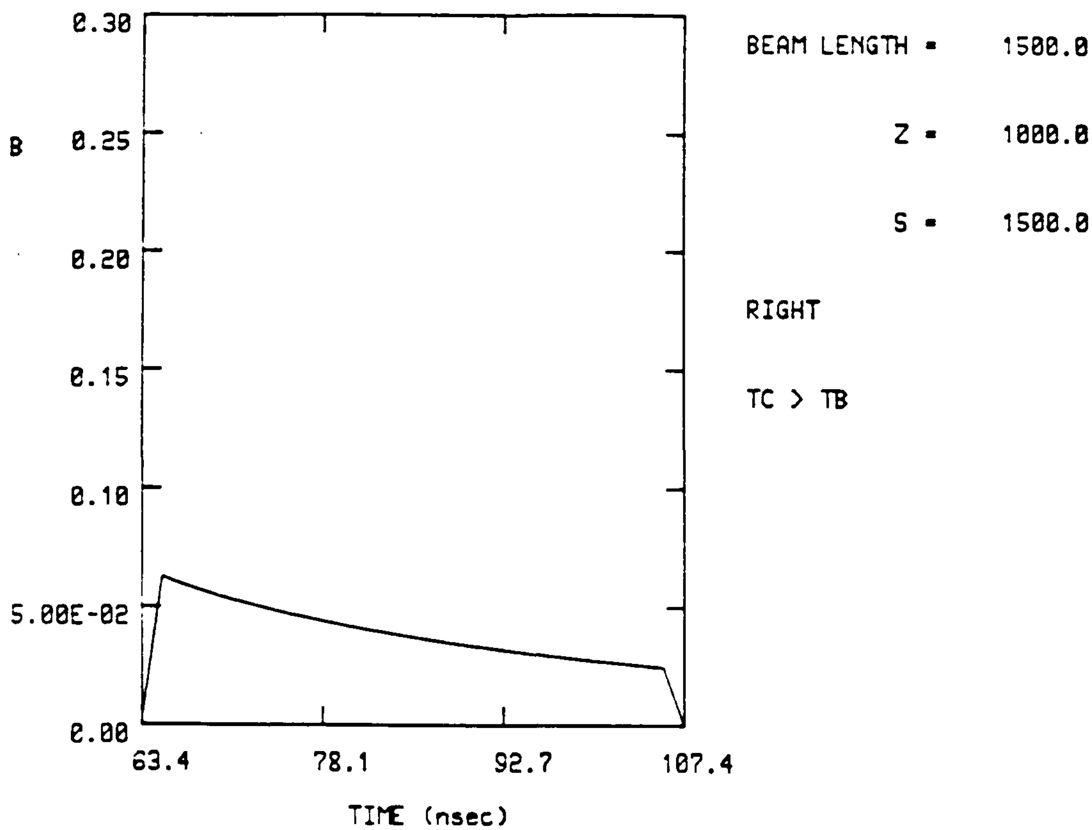

Figure 22: s=1500, z=1000; Tc >TB

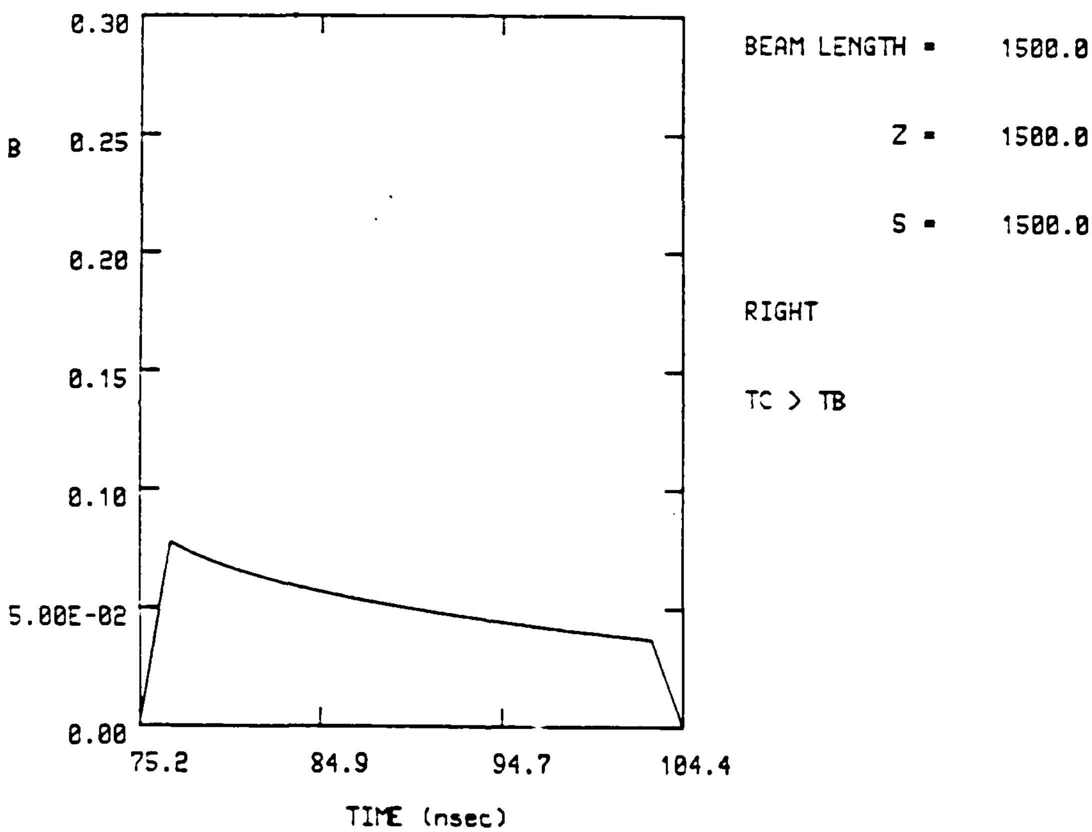

Figure 23: s=1500, z=1500; Tc>TB

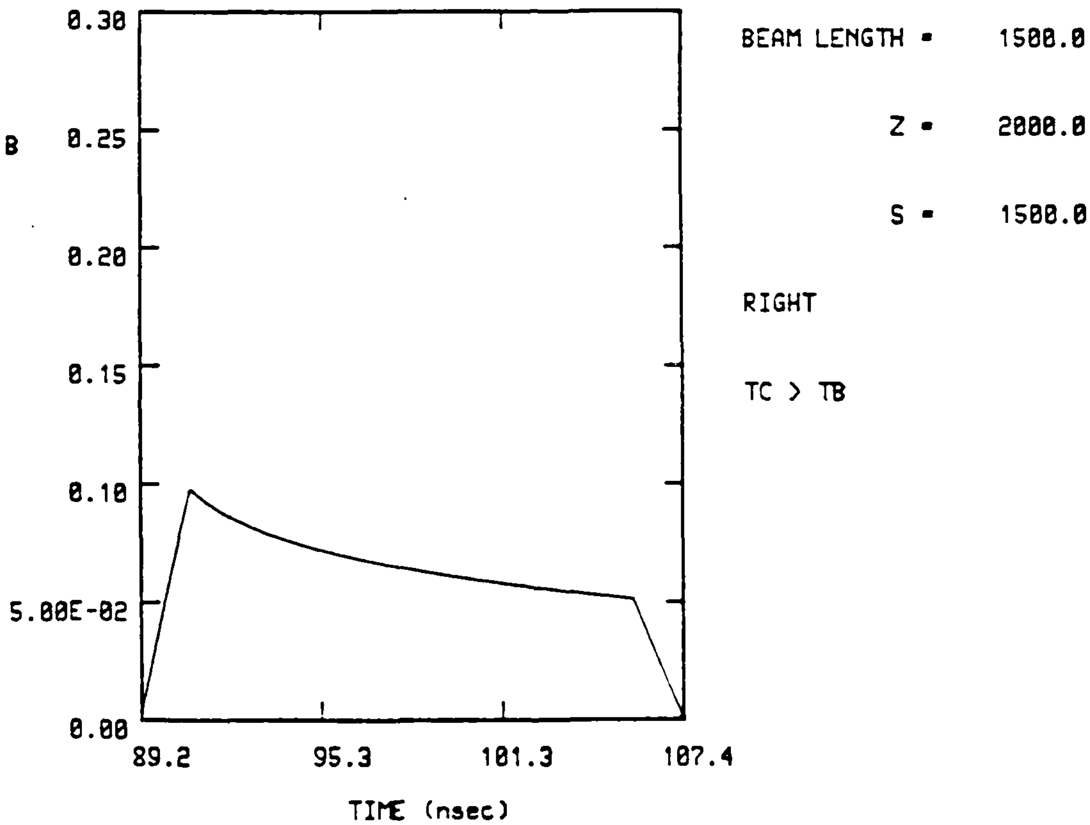

Figure 24: s=1500, z=2000; Tc >Tb

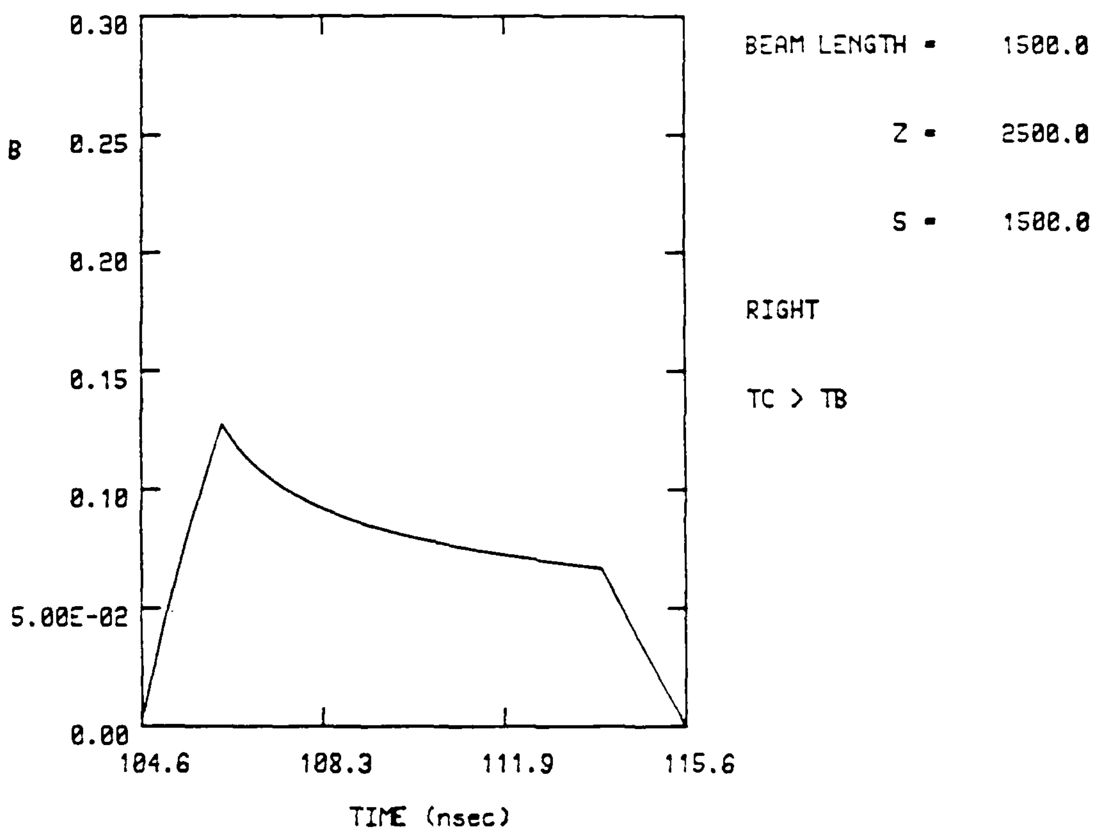

Figure 25: s=1500, z=2500; Tc>TB

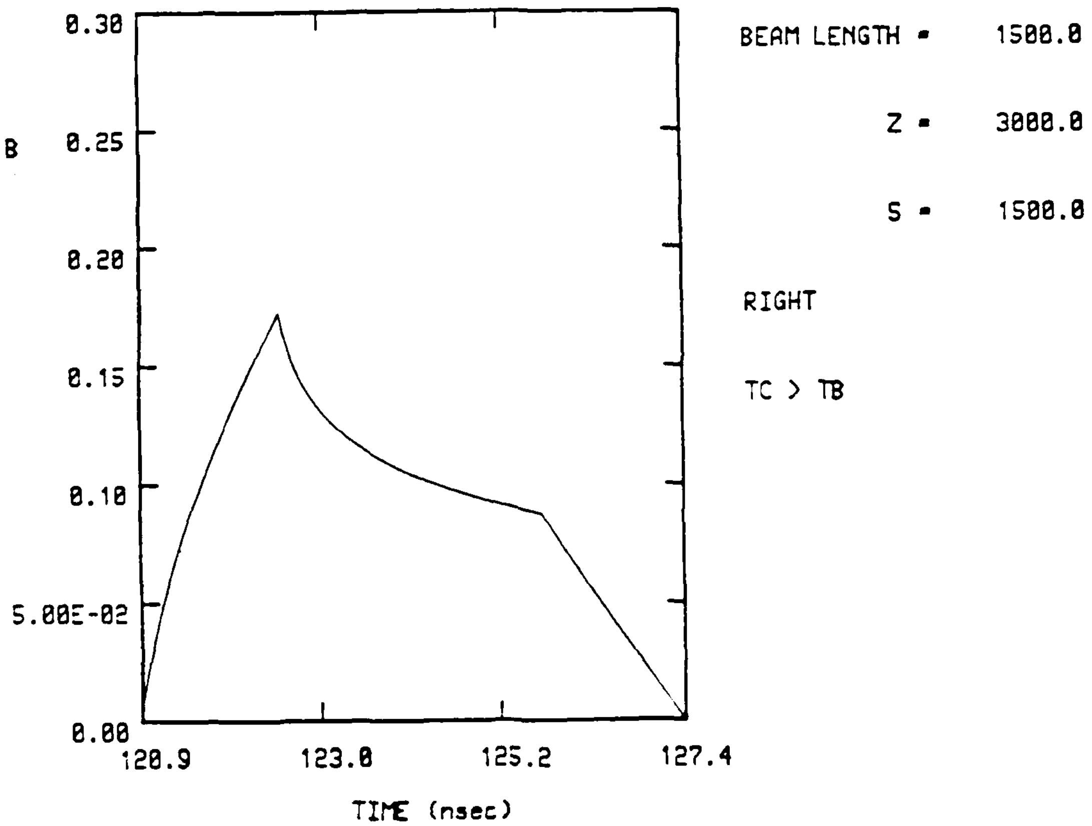

Figure 26: s=1500, z=3000; $T_C > T_B$

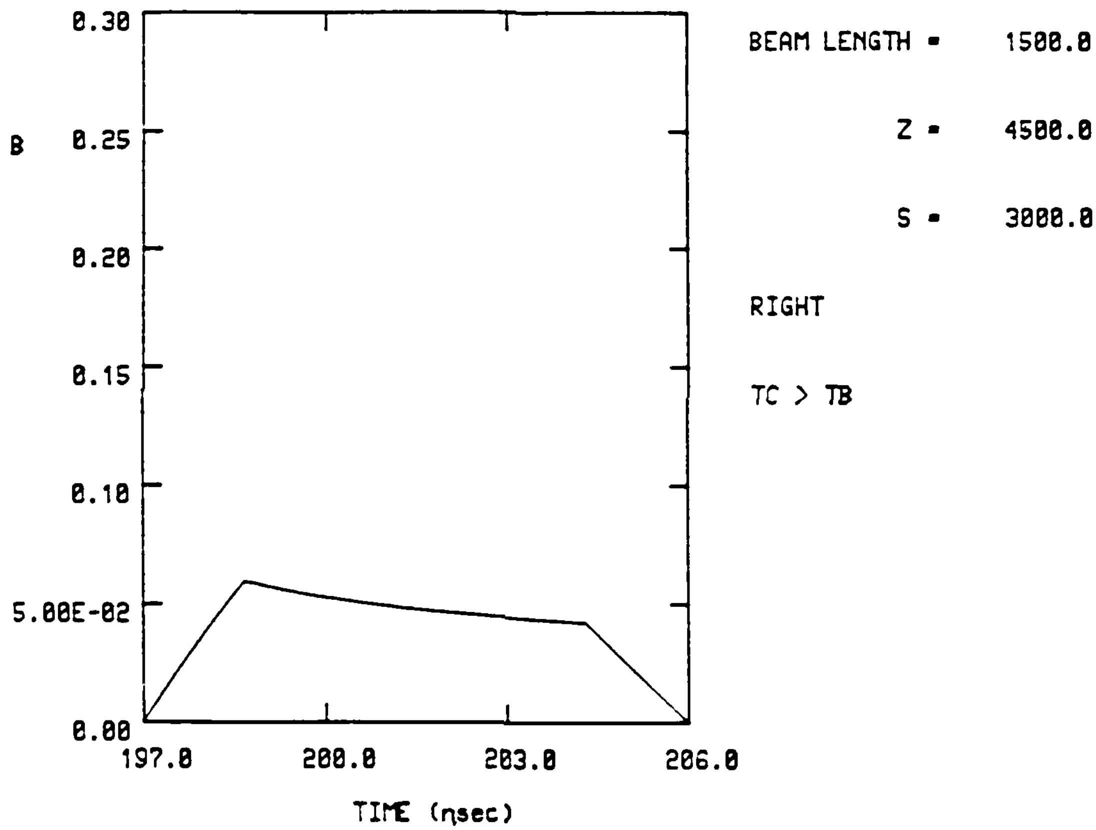

Figure 27: s=3000, z=4500; Tc>Tb

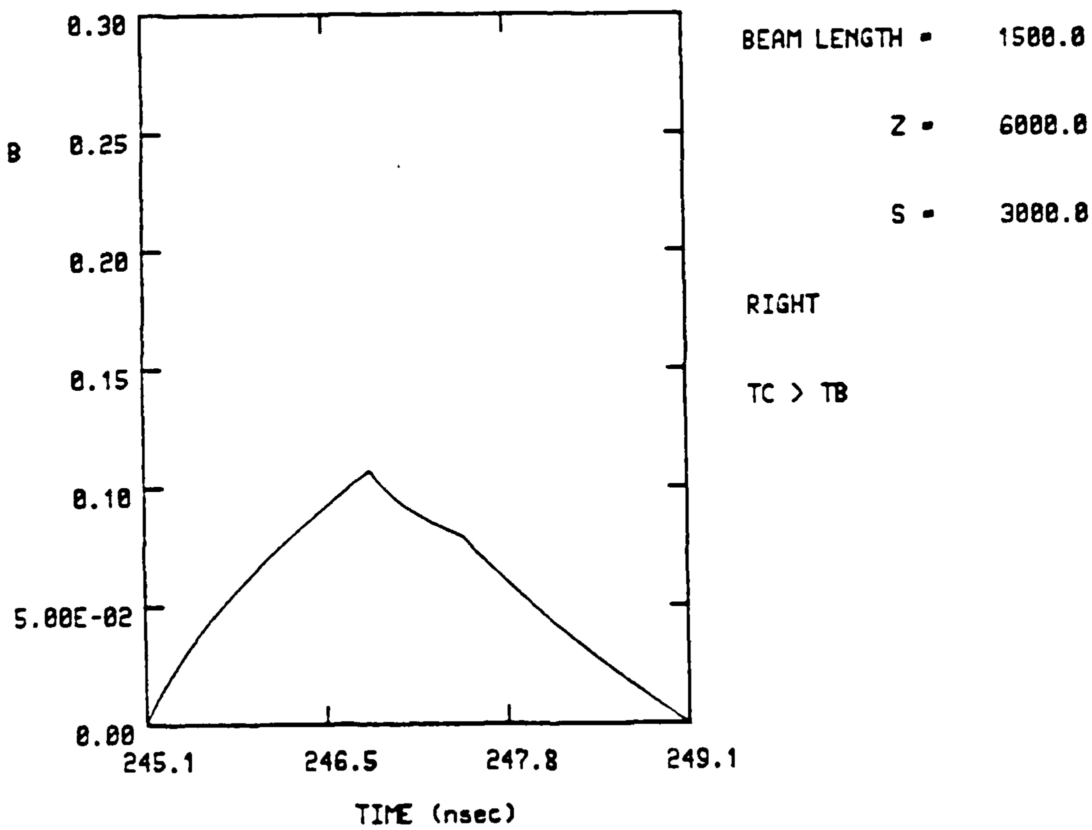

Figure 28: s=3000, z=6000; Tc >TB

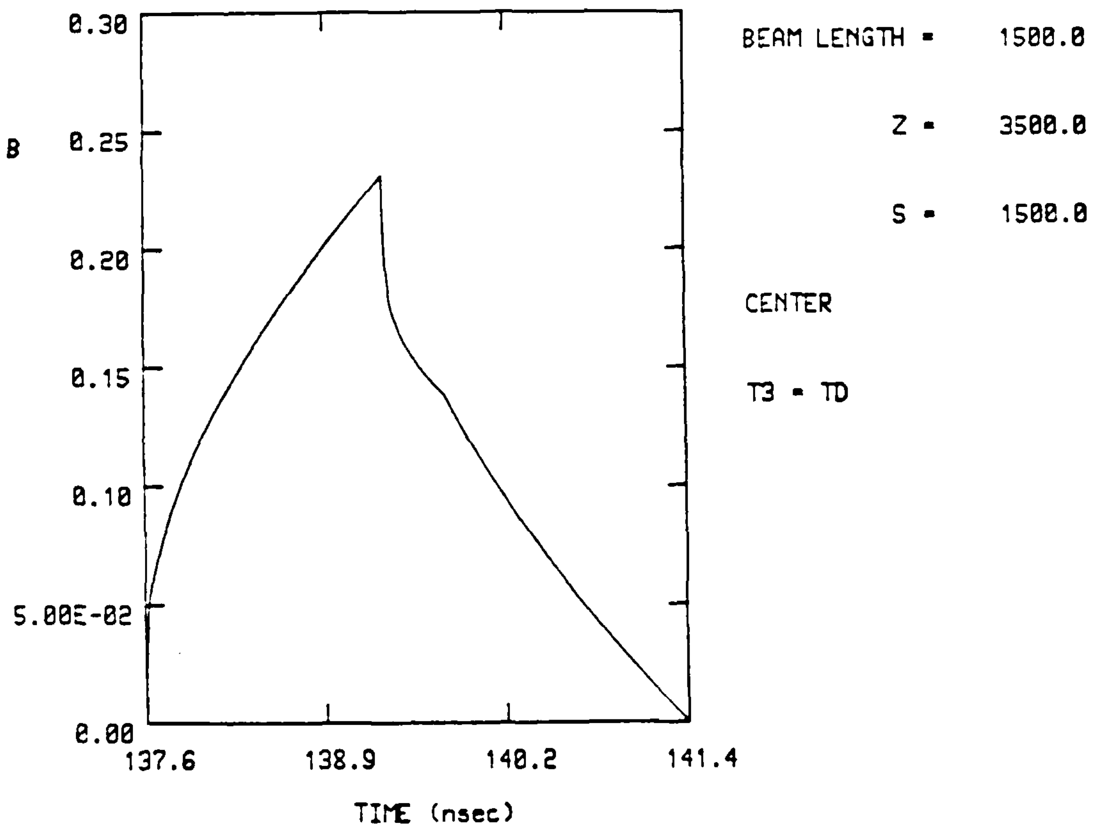

Figure 29: s=1500, z=3500; $T_C > T_B$

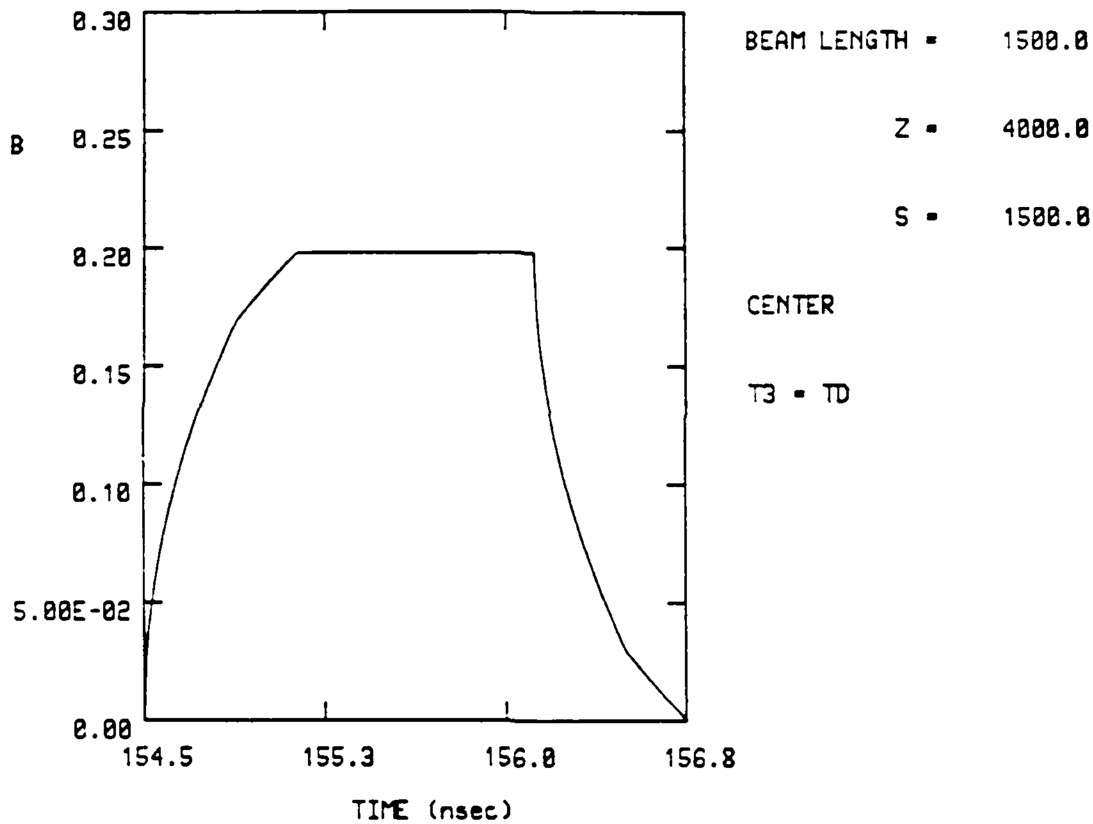

Figure 30: s=1500, z=4000; Time Region Between Lines #1 and #2 of Figure 19

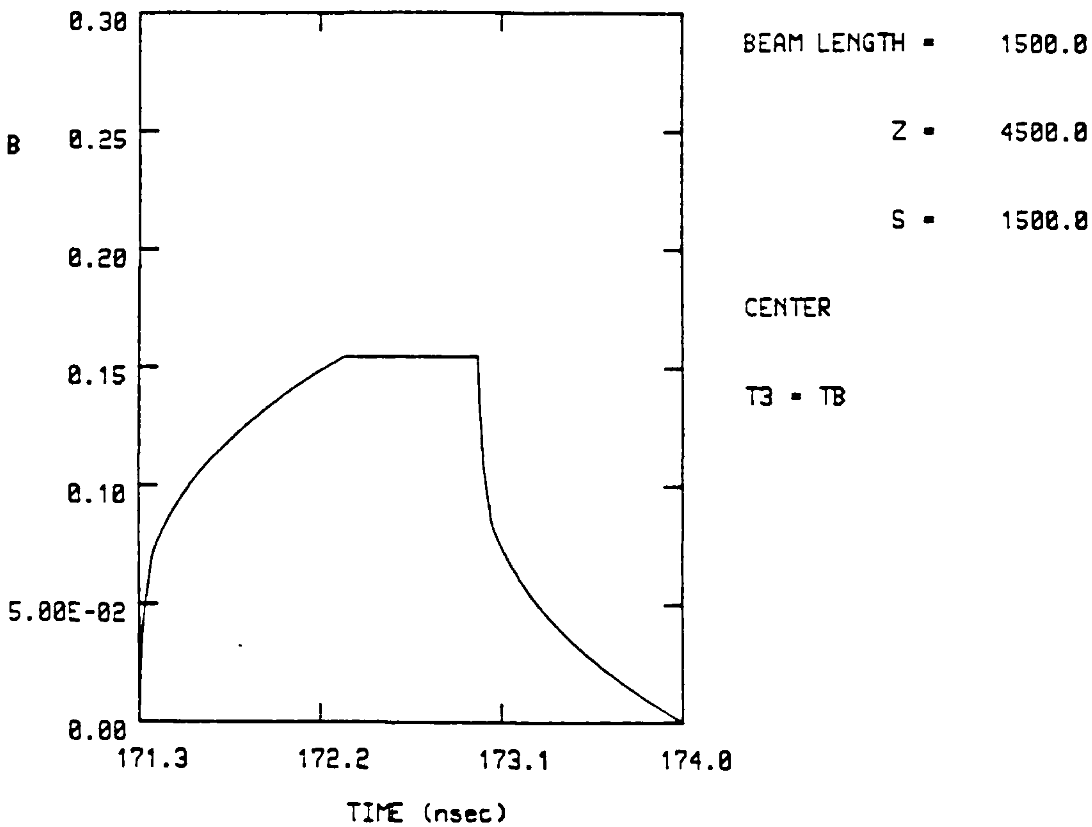

Figure 31: s=1500, z=4500; Time Region Between Lines #1 and #2 of Figure 19

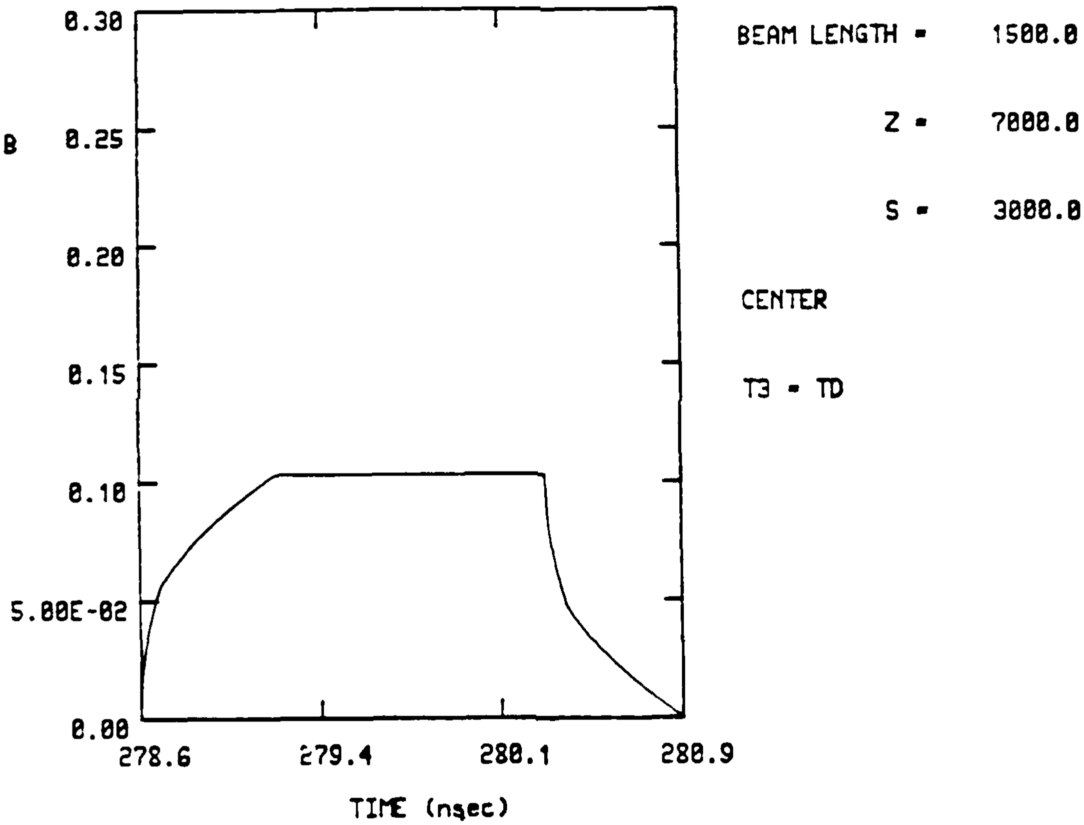

Figure 32: s=3000, z=7000; Time Region Between Lines #1 and #2 of Figure 19

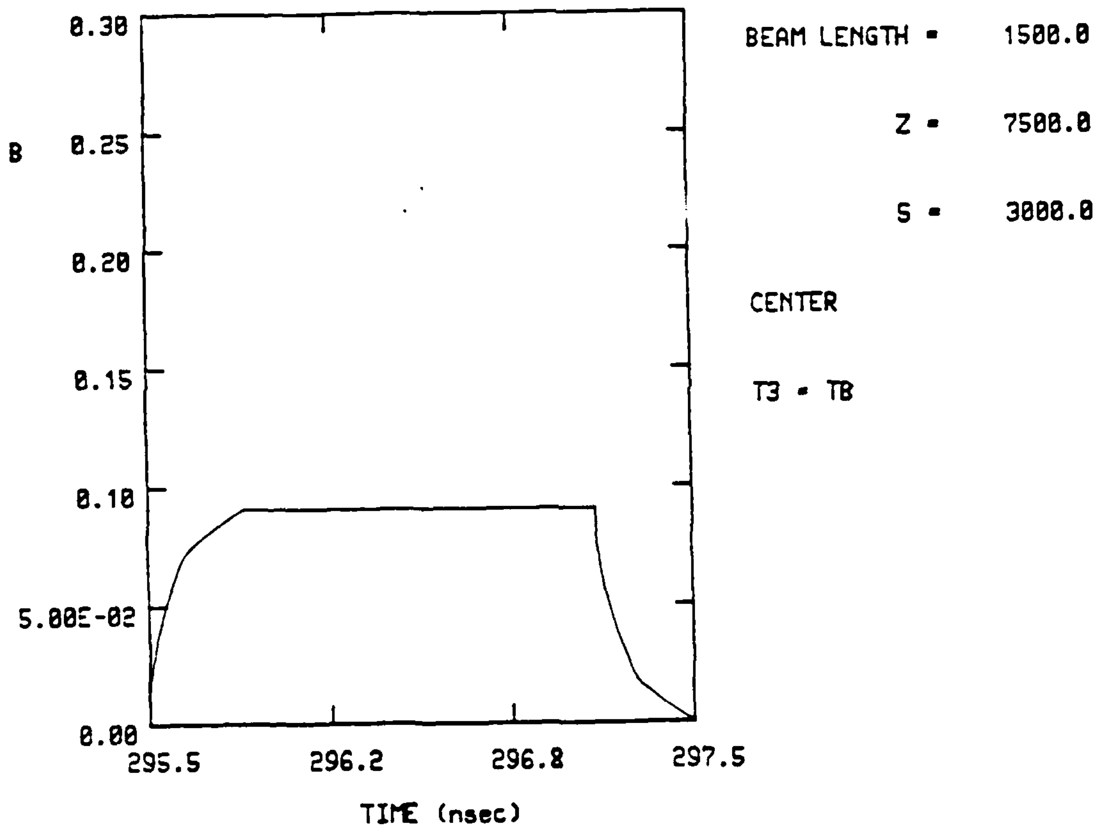

Figure 33: s=3000, z=7500; Time Region Between Lines #1 and #2 of Figure 19

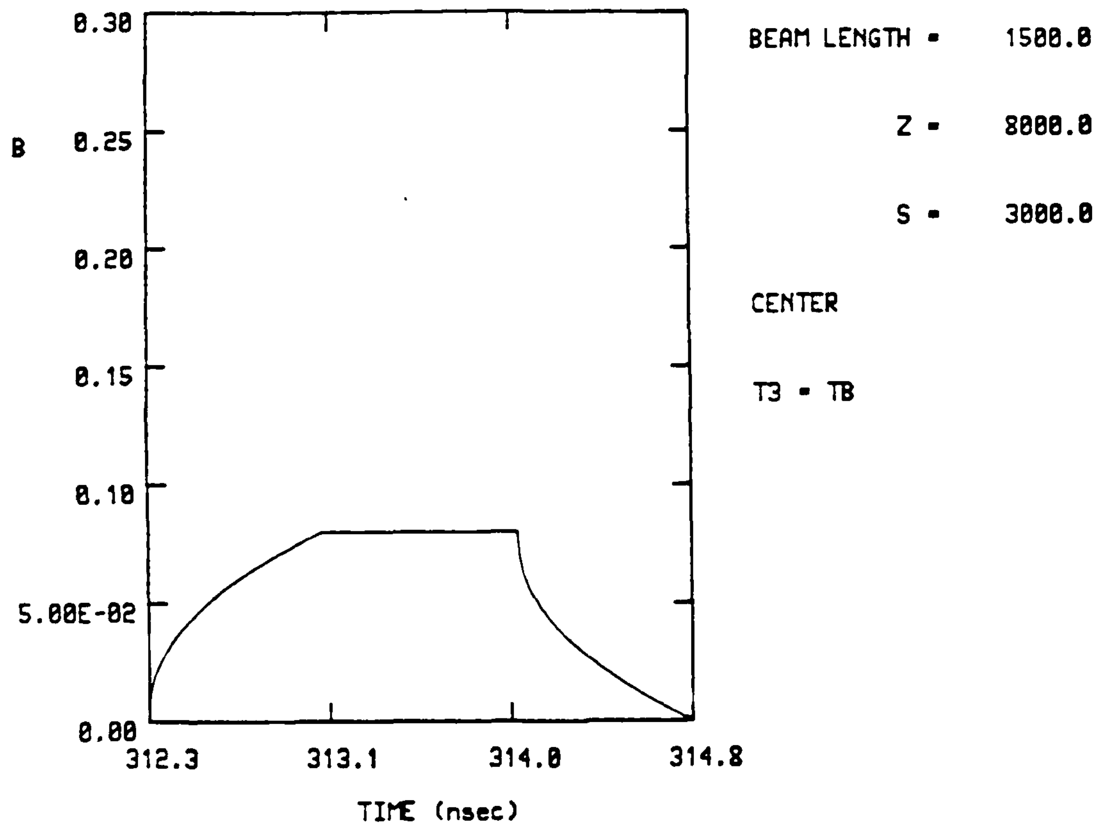

Figure 34: s=3000, z= 8000; Time Region Between Lines #1 and #2 of Figure 19

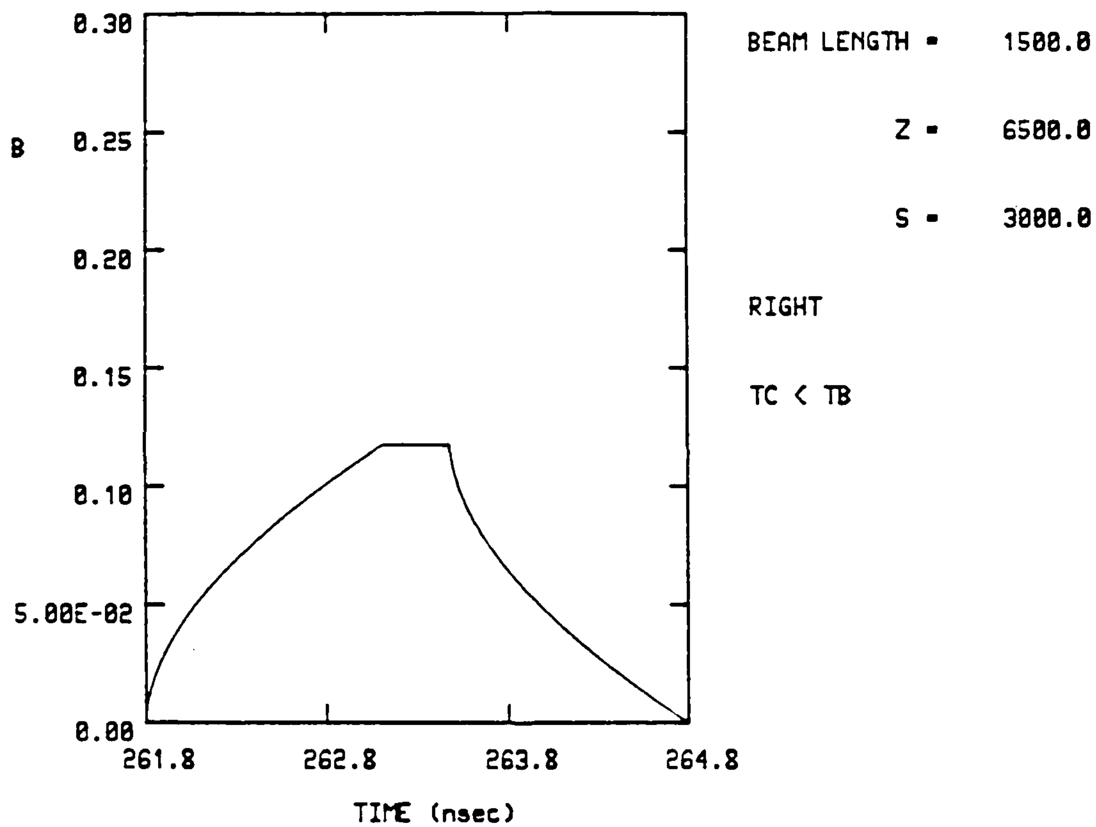

Figure 35: s=3000, z=6500; Time Region Between Lines #1 and #2 of Figure 19

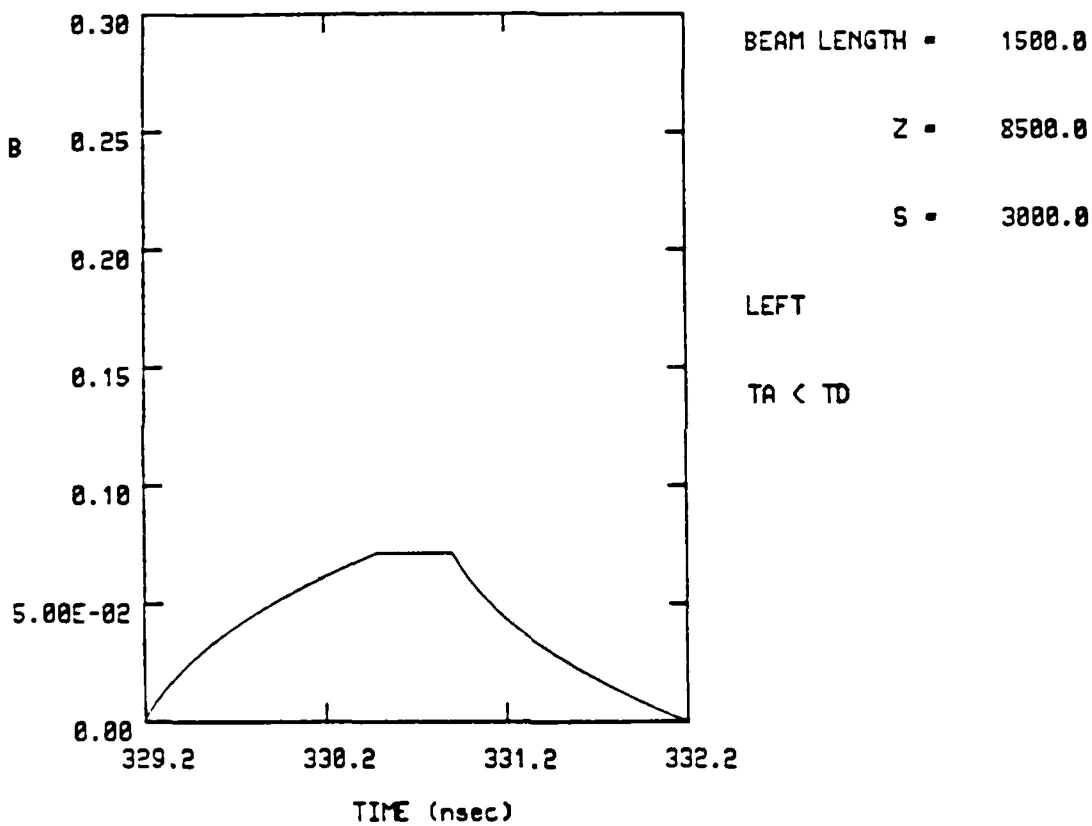

Figure 36: s=3000, z=8500; Time Region Between Lines #1 and #2 of Figure 19

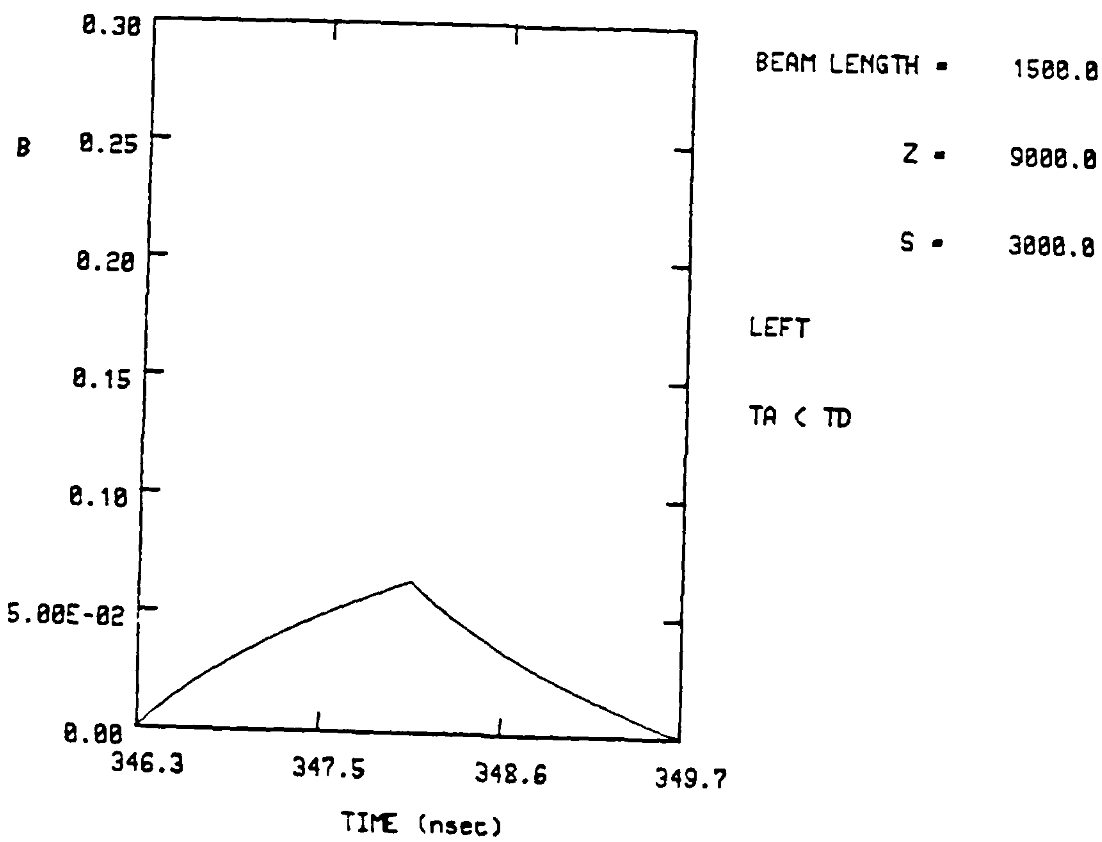

Figure 37: s=3000, z=9000; Time Region Between Lines #1 and #2 of Figure 19

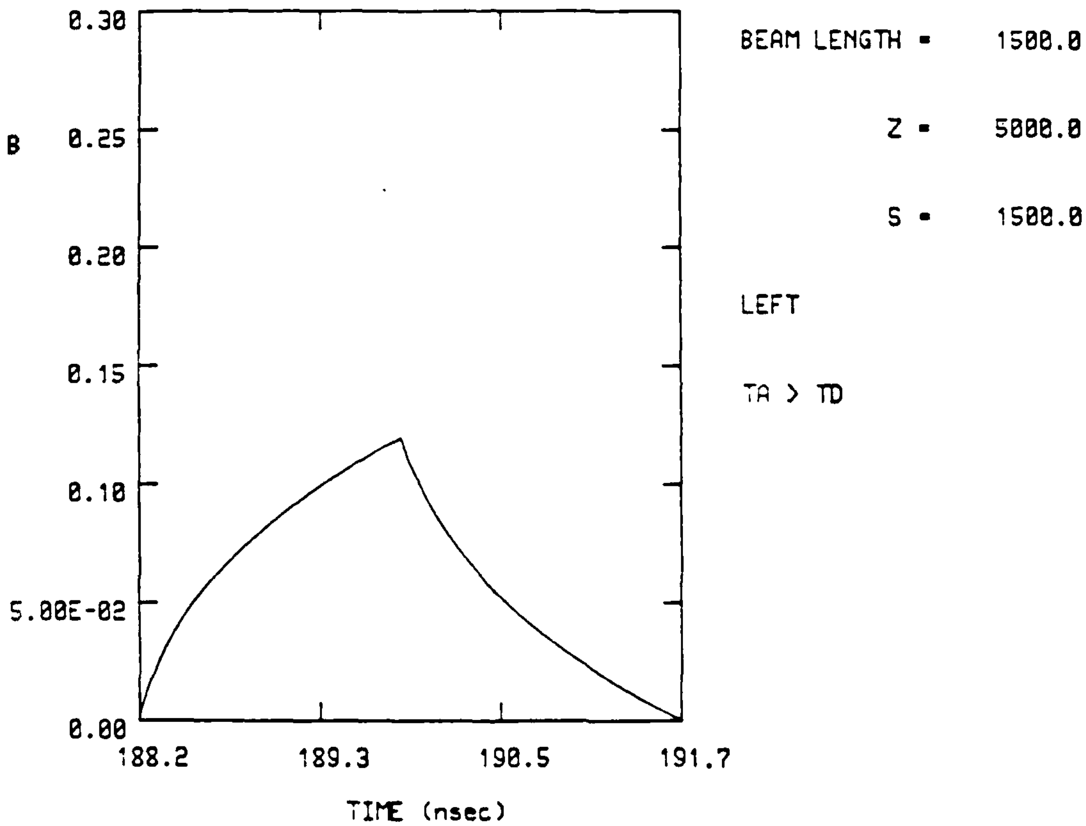

Figure 38: s=1500, z=5000; $T_A > T_D$

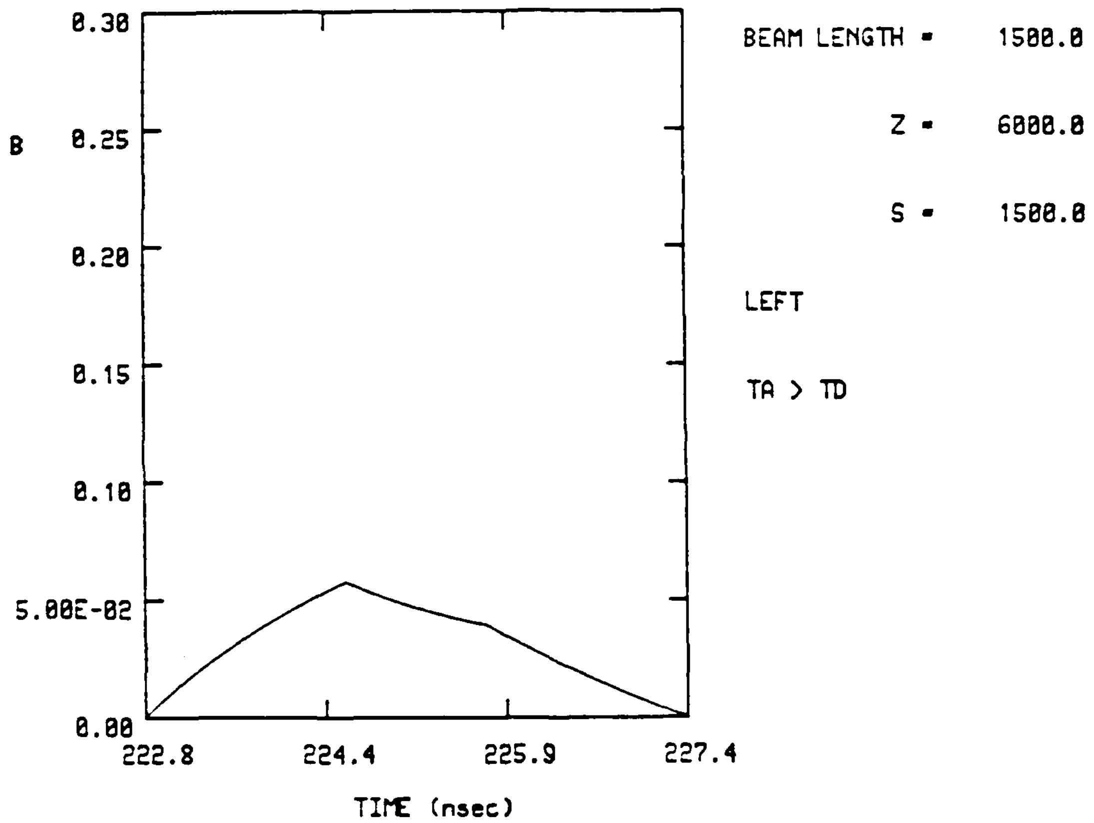

Figure 39: s=1500, z=6000; $T_A > T_D$

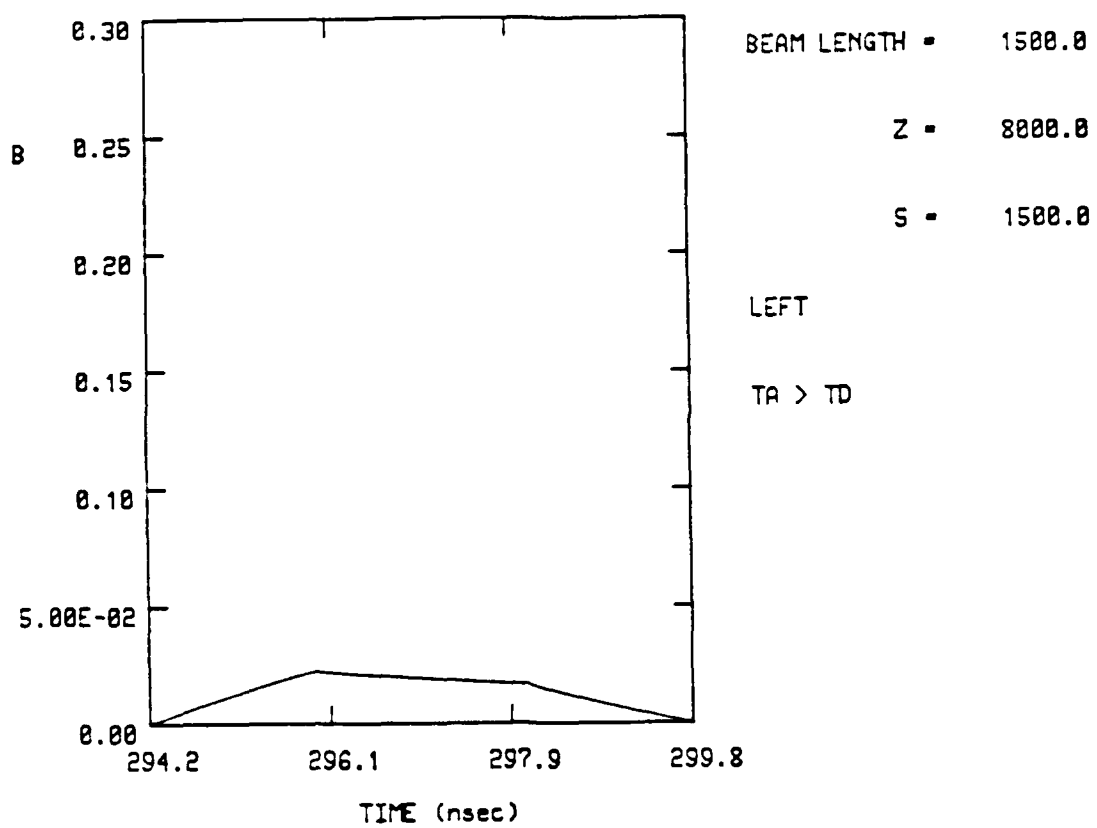

Figure 40: s=1500, z=8000; $T_A > T_D$

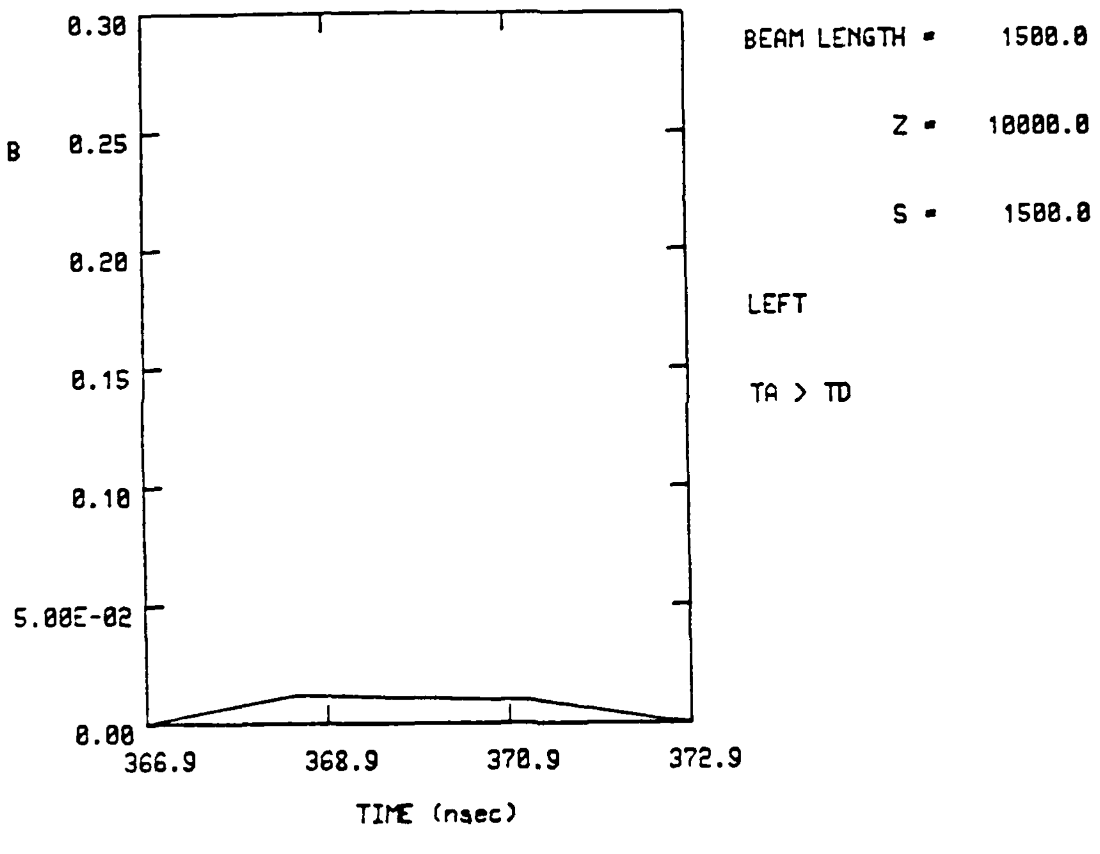

Figure 41: s=1500, z=10000; $T_A > T_D$

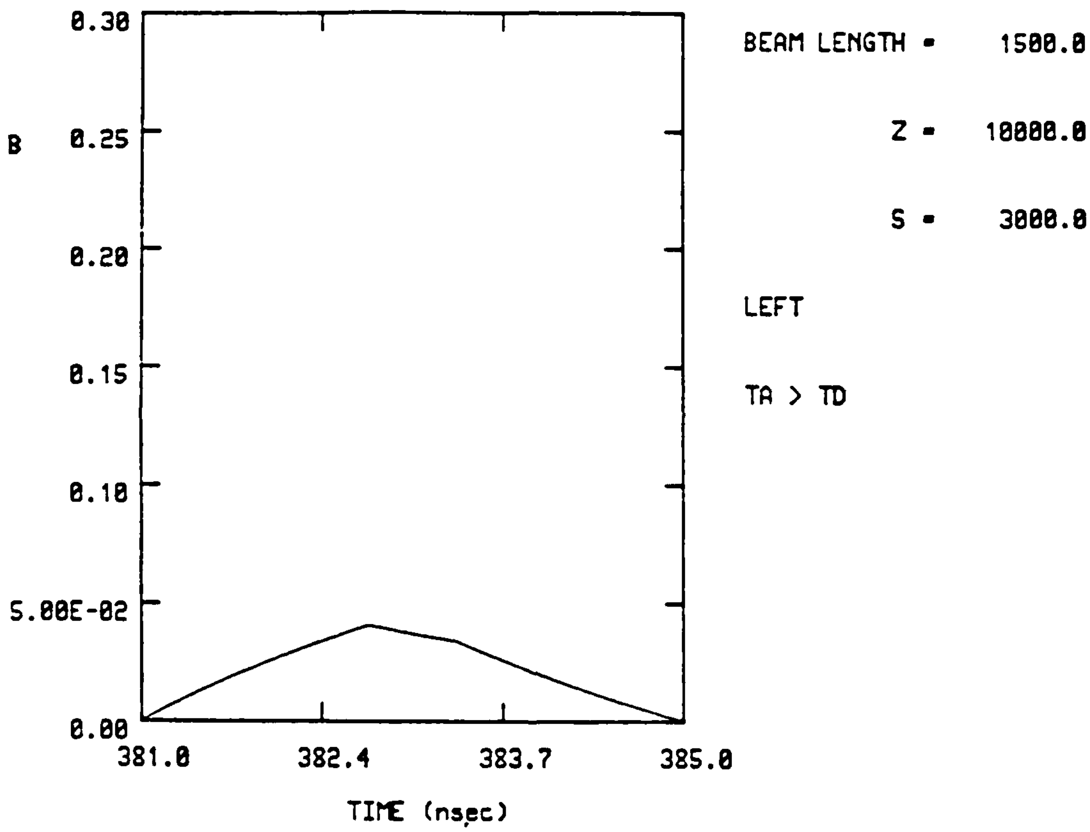

Figure 42: s=3000, z=10000; $T_A > T_D$

APPENDIX B

FORTRAN PROGRAM: FIELDS

```
C******  PROGRAM FIELDS *******

C******  THIS PROGRAM WILL CALCULATE THE FIELDS FROM A
         PASSING CHARGE BUNCH.  IT WAS WRITTEN BY LCDR
         KATHLEEN M. LYMAN, USN; THE GRAPHICS PORTION OF THE
         PROGRAM IS BASED ON CODE WRITTEN BY PROF. J.R.
         NEIGHBOURS OF THE NAVAL POSTGRADUATE SCHOOL.


         REAL N,U1,U2,BETA,CO,ROE,A,G,CE,V,BPRME,R1,R2,A1
         REAL A2,D,E,DD,EE,Q,TA,TB,TC,TD,F,ZPI,ZPF,WPI,WPF
         REAL W1,W2,ZC,RC,ZPC,T1,T2,T3,DELR,ZPM,ZPM2,B1,B2
         REAL E1,E2,S1,XX,YY,S,L,Z,TPRME,B,BMAX,TMAX,XMAX
         REAL SDYY,SDXX,SCALEY,SCALEX,SDX,SDY,SN,YN,YMIN,X,Y
         REAL YMAX,XMIN,TMIN,GPRME,THETA1,THETA2
         DIMENSION TPRME(9000),B(9000)
         INTEGER I,J,JXMAX,JYMAX,IMAX
         CHARACTER*1 AXCH,PRE
         CHARACTER*6 PATH
         CHARACTER*8 TIME

300      WRITE(6,2000)
2000     FORMAT('  U1 =  ',$)
         READ(5,*)U1
         WRITE(6,2001)
2001     FORMAT('  U2 =  ',$)
         READ(5,*)U2
         WRITE(6,2005)
2005     FORMAT('BETA =  ',$)
         READ(5,*)BETA
         WRITE(6,2007)
2007     FORMAT('   N =  ',$)
         READ(5,*)N
         WRITE(6,2009)
2009     FORMAT(' ROE =  ',$)
         READ(5,*)ROE

C******  INITIAL VALUES ********
         DO 900 I = 1,9000
         TPRME(I) = 0.0
900      CONTINUE

         DO 910 I = 1,9000
         B(I) = 0.0
910      CONTINUE
```

```
      TMAX=0.0
      TMIN=0/0
      IMAX=0
      BMAX=0.00000000
      C0=29.997250

C****** CALCULATE THE VELOCITY V AND BETA PRIME (BPRME)
      V=BETA*C0
      BPRME=N*BETA

      Q=BPRME**2.-1.

C****** CALCULATE THE CERENKOV ANGLE (CE) ******
      CE = ACOS(1/BPRME)
      F = TAN(CE)

      WRITE(6,1002)
1002  FORMAT('ENTER S VALUE FOR GRAPH    ',$)
      READ(5,*)S

      WRITE(6,1003)
1003  FORMAT('ENTER L VALUE FOR GRAPH    ',$)
      READ(5,*)L

      WRITE(6,1004)
1004  FORMAT('ENTER Z VALUE FOR GRAPH    ',$)

      R1 = SQRT(S**2.+Z**2.)
      R2 = SQRT(S**2.+(Z-L)**2.)

      S1 = (S**2.)*Q

C****** CALCULATE THE BOUNDARY TIMES *******
      TA = (BPRME*R1-U1)/V
      WRITE(6,3013)TA
3013  FORMAT('TA:',4X,F9.4)

      TB = (BPRME*R1-U2)/V
      WRITE(6,3014)TB
3014  FORMAT('TB:',4X,F9.4)

      TC = (L+(BPRME*R2)-U1)/V
      WRITE(6,3015)TC
3015  FORMAT('TC:',4X,F9.4)

      TD = (L+(BPRME*R2)-U2)/V
      WRITE(6,3016)TD
3016  FORMAT('TD:',4X,F9.4)
```

```
C****** CALULATE THE VALUE OF TAN(THETA 1),(A), AND
C****** THE VALUE OF TAN(THETA 2),(G)
        A=S/Z
        IF(Z.LT.L)GO TO 500
        IF(Z.EQ.L)GO TO 501
        G=S/(Z-L)
        GO TO 502

C****** COMPARISON TO DETERMINE ON WHICH SIDE THE MINIMUM
C****** LIES
500     GPRME=ATAN((L-Z)/S)+90.
        THETA1=ATAN(A)
        THETA2=ATAN(GPRME)
        IF(THETA1.GT.CE)GO TO 10
        IF(THETA2.GE.CE)GO TO 15
        GO TO 20

501     GPRME=90.
        THETA1=ATAN(A)
        IF(THETA1.GT.CE)GO TO 10
        GO TO 15

502     IF(A.GT.F)GO TO 10
        IF(G.GE.F)GO TO 15
        GO TO 20

C****** PATH TO THE RIGHT *******

10      WRITE(6,2050)
2050    FORMAT('PATH TO THE RIGHT')
        PATH='RIGHT'
        TMIN=TA

303     DO 701 I=1,9000
        TPRME(I)=TA+(REAL(I))/100.
        IF(TPREM(I).GE.TD)GO TO 800

        TMAX=MAX(TMAX,TPRME(I))
        IMAX=MAX(IMAX,I)

        A1=U1+V*TPRME(I))
        A2=U2+(V*TPRME(I))
        D=((BPRME**2.)*Z)-A1
        DD=((BPRME**2.)*Z)-A2
        E1=((Z-A1)**2.)-S1
        E2=((Z-A2)**2.)-S1

        IF(TC.GT.TB)GO TO 25
        IF(TC.LT.TB)GO TO 30
        IF(TC.EQ.TB)GO TO 35
```

```
C****** TC > TB:  CALCULATION OF LIMITS OF INTEGRATION
25      TIME='TC >TB'
        IF((TA.LT.TPRME(I)).AND.(TPRME(I).LT.TB))GO TO 26
        IF((TB.LT.TPRME(I)).AND.(TPRME(I).LT.TC))GO TO 27
        IF((TC.LT.TPRME(I)).AND.(TRPME(I).LT.TD))GO TO 28

C****** TA <T'<TB
26      ZPI=0.
        IF(E1.LT.0.)GO TO 200
        E=BPRME*SQRT(E1)
        ZPF=(D+E)/Q
        IF(ZPF.LT.0.)GO TO 303
        GO TO 101

C****** TB<T'<TC
27      IF(E1.LT.0.)GO TO 200
        E=BPRME*SQRT(E1)
        IF(E2.LT.0.)GO TO 220
        EE=BPRME*SQRT(E2)
        ZPI=(DD+EE)/Q
        ZPF=(D+E)/Q
        IF(ZPI.LT.0.)GO TO 303
        IF(ZPF.LE.0.)GO TO 303
        GO TO 101

C****** TC<T'<TD
28      IF(E2.LT.0.)GO TO 220
        EE=BPRME*SQRT(E2)
        ZPI=(DD+EE)/Q
        ZPF=L
        IF(ZPI.LT.0.)GO TO 303
        GO TO 101

C****** TC < TB:  CALCULATION OF LIMITS OF INTEGRATION
30      TIME='TC < TB'
        IF((TA.LT.TPRME(I)).AND.(TPRME(I).LT.TC))GO TO 31
        IF((TC.LT.TPRME(I)).AND.(TPRME(I).LT.TB))GO TO 32
        IF((TC.LT.TPRME(I)).AND.(TPRME(I).LT.TD))GO TO 33

C****** TA<T'<TC
31      ZPI=0
        IF(E1.LT.0.)GO TO 200
        E=BPRME*SQRT(E1)
        ZPF=(D+E)/Q
        IF(ZPF.LT.0.)GO TO 303
        GO TO 101

C****** TC<T'<TB
32      ZPI=0.
        ZPF=L
        GO TO 101
```

```
C****** TB<T'<TD
33      IF(E2.LT.0.)GO TO 220
        EE=BPRME*SQRT(E2)
        ZPI=(DD+EE)/Q
        ZPF=L
        IF(ZPI.LT.0.)GO TO 303
        GO TO 101

C****** TC = TB:  CALCULATION OF LIMITS OF INTEGRATION
35      TIME='TC = TB'
        IF((TA.LT.TPRME(I)).AND.(TPRME(I).LT.TB))GO TO 36
        IF((TB.LT.TPRME(I)).AND.(TPRME(I).LT.TD))GO TO 37

C****** TA<T'<TB
36      ZPI=0.
        IF(E1.LT.0.)GO TO 200
        E=BPRME*SQRT(E1)
        ZPF=(D+E)/Q
        IF(ZPF.LT.0.)GO TO 303
        GO TO 101

C****** TB<T'<TD
37      IF(E2.LT.0.)GO TO 220
        EE=BPRME*SQRT(E2)
        ZPI=(DD+EE)/Q
        ZPF=L
        IF(ZPF.LT.0.)GO TO 303
        GO TO 101

C****** CALCULATION OF THE FIELD
101     WPI=Z-ZPI
        WPF=Z-ZPF
        W1=WPI/S
        W2=WPF/S
        YY=ATAN(W1)
        XX=ATAN(W2)
        B(I)=(ROE*N*(BETA**2))*(YY-XX)
        BMAX=MAX(BMAX,B(I))
701     CONTINUE
        GO TO 800

C****** PATH CENTERED ABOUT THE MINIMUM ******
15      WRITE(6,2051)
2051    FORMAT('CENTER')
        PATH='CENTER'
        ZPC=Z-(S/F)
        RC=SQRT(S**2.+((Z-ZPC)**2.))

C****** CALCUATION OF T1 AND T2
        T1=(ZPC+(BPRME*RC)-U1)/V
        T2=(ZPC+(BPRME*RC)-U2)/V
        DELR=R1-R2
```

```
      WRITE(6,6000)T1
6000  FORMAT('T1= ',F9.4)
      WRITE(6,6001)T2
6001  FORMAT('T2= ',F9.4)

C****** DETERMINING THE VALUE OF T3
      IF((BPRME*DELR).GT.L)GO TO 16
      IF((BPRME*DELR).LE.L)GO TO 17
16    T3=TB
      TIME='T3 = TB'
      GO TO 18
17    T3=TD
      TIME='T3 = TD'
18    WRITE(6,6002)T3
6002  FORMAT('T3= ',F9.4)

      TMIN=T1
      DO 702 I=1,9000
      TPRME(I)=T1+(REAL(I))/100.
      IF(TPRME(I).GE.T3)GO TO 800
      TMAX=MAX(TMAX,TPRME(I))
      IMAX=MAX(IMAX,I)

      IF((T1.LT.TPRME(I)).AND.(TPRME(I).LT.T2))GO TO 60
      IF((T2.LT.TPRME(I)).AND.(TPRME(I).LT.T3))GO TO 70

C****** CALCULATION OF LIMITS OF INTEGRATION (T1<T'<T2)
60    A1=U1+(V*TPRME(I))
      A2=U2+(V*TPRME(I))
      D=((BPRME**2.)*Z)-A1
      DD=((BPRME**2.)*Z)-A2
      E1=((Z-A1)**2.)-S1
      E2=((Z-A2)**2.)-S1

      IF(E1.LT.0.)GO TO 200
      E=BPRME*SQRT(E1)
      ZPM=(D-E)/Q
      ZPF=(D+E)/Q
      IF(ZPM.LE.0.)GO TO 61
      IF(ZPM.GT.0.)GO TO 62
61    ZPM=0.
62    ZPI=ZPM
63    IF(ZPF.GE.L)GO TO 64
      IF(ZPF.GT.L)GO TO 110
64    ZPF=L

C****** CALCULATION OF THE FIELD
110   WPI=Z-ZPI
      WPF=Z-ZPF
      W1=WPI/S
      W2=WPF/S
      YY=ATAN(W1)
```

```
      XX=ATAN(W2)
      B(I)=(ROE*N*(BETA**2.))*(YY-XX)
      BMAX=MAX(BMAX,B(I))
      GO TO 702

C****** CALCULATION OF LIMITS OF INTEGRATION (T2<T'<T3)

C****** FIRST INTEGRAL
70    A1=U1+(V*TPRME(I))
      A2=U2+(V*TPRME(I))
      D=((BPRME**2.)*Z)-A1
      DD=((BPRME**2.)*Z)-A2
      E1=((Z-A1**2.)-S1
      E2=((Z-A2**2.)-S1

      IF(E1.LT.0.)GO TO 200
      E=BPRME*SQRT(E1)
      IF(E2.LT.0.)GO TO 220
      EE=BPRME*SQRT(E2)
      ZPM=(D-E)/Q
      ZPM2=(DD-EE)/Q
      IF(ZPM2.LE.0.)GO TO 73
      IF(ZPM2.GT.0.)TO TO 74
73    ZPF=0.
      GO TO 75
74    ZPF=ZPM2
75    IF(ZPM.LE.0)GO TO 71
      IF(ZPM.GT.0)GO TO 72
71    ZPI=0.
      GO TO 80
72    ZPI=ZPM

C****** CALCULATION OF THE FIELD FROM THE FIRST INTEGRAL
80    WPI=Z-ZPI
      WPF=Z-ZPF
      W1=WPI/S
      W2=WPF/S
      YY=ATAN(W1)
      XX=ATAN(W2)
      B1=(ROE*N*(BETA**2.))*(YY-XX)

C****** SECOND INTEGRAL
      IF(E1.LT.0.)GO TO 200
      E=BPRME*SQRT(E1)
      IF(E2.LT.0.)GO TO 220
      EE=BPRME*SQRT(E2)
      ZPI=(DD+EE)/Q
      ZPF=(D+E)/Q
```

```
      IF(ZPI.GE.L)GO TO 83
      GO TO 84
83    ZPI=L
84    IF(ZPF.GE.L)GO TO 82
      IF(ZPF.LT.L)GO TO 81
82    ZPF=L

C****** CALCULATION OF THE FIELD FROM THE SECOND INTEGRAL
81    WPI=Z-ZPI
      WPF=Z-ZPF
      W1=WPI/S
      W2=WPF/S
      YY=ATAN(W1)
      XX=ATAN(W2)
      B2=(ROE*N*(BETA**2.))*(YY-XX)

C****** TOTAL FIELD
      B(I)=B1+B2

      BMAX=MAX(BMAX,B(I))
702   CONTINUE
      GO TO 800

C****** PATH TO THE LEFT
20    WRITE(6,2052)
2052  FORMAT('PATH TO THE LEFT')
      PATH='LEFT'
      TMIN=TC

304   DO 700 I=1,9000
      TPRME(I)=(TC+REAL(I))/100.
      IF TPRME(I).GE.TB)GO TO 800
      TMAX=MAX(TMAX,TPRME(I))
      IMAX=MAX(IMAX,I)

      A1=U1+(V*TPRME(I))
      A2=U2+(V*TPRME(I))
      D=((BRPME**2.)*Z)-A1
      DD=((BPRME**2.)*Z)-A2
      E1=(Z-A1)**2.-S1
      E2=(Z-A2)**2.-S1

      IF(TA.LT.TD)GO TO 40
      IF(TA.GT.TD)GO TO 45
      IF(TA.EQ.TD)GO TO 50

C****** TA < TD:  CALCULATION OF LIMITS OF INTEGRATION
40    TIME='TA < TD'
      IF((TC.LT.TPRME(I)).AND.(TPRME(I).LT.TA))GO TO 41
      IF((TA.LT.TPRME(I)).AND.(TPRME(I).LT.TD))GO TO 42
      IF((TA.LT.TPRME(I)).AND.(TPRME(I).LT.TB))GO TO 43
```

```
C****** TC<T'<TA
41      IF(E1.LT.0.)GOTO 200
        E=BPRME*SQRT(E1)
        ZPM=(D-E)/Q
        ZPF=L
        ZPI=ZPM
        IF(ZPI.LT.0.)GO TO 304
        GO TO 100

C****** TA<T'<TD
42      ZPI=0.
        ZPF=L
        GO TO 100
C****** TA<T'<TB
43      ZPI=0.
        IF(E2.LT.0.)GO TO 220
        EE=BPRME*SQRT(E2)
        ZPM2=(DD-EE)/Q
        ZPF=ZPM2
        IF(ZPF.LT.0.)GO TO 304
        GO TO 100

C****** TA > TD:  CALCULATION OF LIMITS OF INTEGRATION
45      TIME='TA > TD'
        IF((TC.LT.TPRME(I)).AND.(TPRME(I).LT.TD))GO TO 46
        IF((TD.LT.TPRME(I)).AND.(TPRME(I).LT.TA))GO TO 47
        IF((TA.LT.TPRME(I)).AND.(TPRME(I).LT.TB))GO TO 48

C****** TC<T'<TD
46      IF(E1.LT.0.)GO TO 200
        E=BPRME*SQRT(E1)
        ZPM=(D-E)/Q
        ZPF=L
        ZPI=ZPM
        IF(ZPI.LT.0.)GO TO 304
        GO TO 100

C****** TD<T'<TA
47      IF(E1.LT.0.)GO TO 200
        E=BPRME*SQRT(E1)
        IF(E2.LT.0.)GO TO 220
        EE=BPRME*SQRT(E2)
        ZPM=(D-E)/Q
        ZPM2=(DD-EE)/Q
        ZPI=ZPM
        ZPF=ZPM2
        IF(ZPI.LT.0.)GO TO 304
        IF(ZPF.LT.0.)GO TO 304
        GO TO 100
```

```
C****** TA<T'<TB
48      ZPI=0.
        IF(E2.LT.0.)GO TO 220
        EE=BPRME*SQRT(E2)
        ZPM2=(DD-EE)/Q
        ZPF=ZPM2
        IF(ZPF.LT.0.)GO TO 304
        GO TO 100

C****** TA = TD:  CALCULATION OF LIMITS OF INTEGRATION
50      TIME='TA = TD'
        IF((TC.LT.TPRME(I)).AND.(TPRME(I).LT.TA))GO TO 51
        IF((TD.LT.TPRME(I)).AND.(TPRME(I).LT.TB))GO TO 52

C****** TC<T'<TA
51      IF(E1.LT.0.)GO TO 200
        E=BPRME*SQRT(E1)
        ZPM=(D-E)/Q
        ZPF=L
        ZPI=ZPM
        IF(ZPI.LT.0.)GO TO 304
        GO TO 100

C****** TD<T'<TB
52      ZPI=0.
        IF(E2.LT.0.)GO TO 220
        EE=BPRME*SQRT(E2)
        ZPM2=(DD-EE)/Q
        ZPF=ZPM2
        IF(ZPF.LT.0.)GO TO 304
        GO TO 100

C****** CALCULATION OF THE FIELD
100     WPI=Z-ZPI
        WPF=Z-ZPF
        W1=WPI/S
        W2=WPF/S
        YY=ATAN(W1)
        XX=ATAN(W2)
        B(I)=(ROE*N*(BETA**2.))*(YY-XX)
        BMAX=MAX(BMAX,B(I))
700     CONTINUE

200     WRITE(6,201)
201     FORMAT('VALUE OF E1 IS NEGATIVE.  PROGRAM WILL BEGIN
              AGAIN.')
        GO TO 300

220     WRITE(6,221)
221     FORMAT('VALUE OF E2 IS NEGATIVE.  PROGRAM WILL BEGIN
              AGAIN.')
        GO TO 300
```

```
C****** BEGIN GRAPHICS ************
C****** INPUT SCALING VALUES ******
800     WRITE(6,1510)BMAX
1510    FORMAT(/'THE MAXIMUM VALUE OF B IS   ',F16.8)
        WRITE(6,1520)
1520    FORMAT(/'ENTER THE MAXIMUM HEIGHT ON THE B AXIS'.$)
        READ(5,*)YMAX
        WRITE(6,1530)
1530    FORMAT(/'ENTER THE B AXIS MARKING INCREMENT  ',$)
        READ(5,*)SDYY
        CALL INETYPE(IPAT)
        CALL COLORLIN(ICOLOR)

        WRITE(6,1560)
1560    FORMAT('DO YOU WANT INFORMATION PRINTED ALONGSIDE
                THE GRAPH?   ',$)
        READ(5,1570)AXCH
A570    FORMAT(A1)

        CALL INSTR1
        PAUSE'#1'

        XMAX=TMAX
        XMIN=TMIN
        SDXX=(TMAX-TMIN)/3.0
        SCALEX=60.0/(XMAX-XMIN)
        SDX=SDXX*SCALEX
        XN=(XMAX-XMIN)/SDXX
        JXMAX=INT(XN)

        YMIN=0.0
        SCALEY=80.0/(YMAX-YMIN)
        SDY=SCALEY*SDYY
        YN=(YMAX-YMIN)/SDYY
        JYMAX=INT(YN)

C****** BEGIN TO PLOT ******
        CALL GRSTRT(4105,1)
        CALL NEWPAG
        CALL VAXES
        CALL VXMARK(JXMAX,SDX)
        CALL VYMARK(JYMAX,SDY)

C****** PLOT GRAPH ******
        CALL MOVE(18.0,19.0)
        CALL DASHPT(IPAT)
        CALL LINCLR

        DO 540 I=1,IMAX
C****** SCALING OF VALUES ******
        X=18.0+60.0*((TPRME(I)-TMIN)*100.)/IMAX
        Y=19.0+80.0*B(I)/YMAX
```

```
      CALL DRAW(X,Y)
540   CONTINUE
C****** DECISION TO LABEL GRAPH ******
      CALL GRSTOP
      CALL INSTR2
      PAUSE'#3'
      CALL LINE
      CALL INSTR1
      PAUSE'#4'
      CALL GRSTRT(4105,1)

      CALL XLABEL(JXMAX,SDX,SDXX,XMIN)
      CALL YLABEL(JYMAX,SDY,SDYY,YMIN)
C****** AXES LABELS AND PARAMETER LEGEND ******
      IF(AXCH.EQ.'Y')GO TO 556
      GO TO 651
556   CALL MOVE(50.0,10.0)
      CALL TXICUR(8)
      CALL TEXT(11,'TIME (NSEC)')
      CALL MOVE(5.0,83.0)
      CALL TXICUR(3)
      CALL TEXT(1,'B')
      REL=REAL(L)
      RES=REAL(S)
      REZ=REAL(Z)
      CALL MOVE(85.0,95.0)
      CALL TXICUR(1)
      CALL TXFCUR(2)
      CALL TEXT(15,'BEAM LENGTH = ')
      CALL RNUMBR(REL,1,8)
      CALL MOVE(85.0,85.0)
      CALL TEXT(15,'           Z = ')
      CALL RNUMBR(REZ,1,8)
      CALL MOVE(85.0,75.0)
      CALL TEXT(15,'           S = ')
      CALL RNUMBR(RES,1,8)
      CALL MOVE(85.0,65.0)
      CALL TEXT(6,PATH)
      CALL MOVE(85.0,55.0)
      CALL TEXT(8,TIME)

651   CALL GRSTOP
      CALL INSTR2
      PAUSE'#5'
      GO TO 440

C****** DECISION TO PRINTOUT, RE-RUN, PLOT VALUES OR EXIT
440   WRITE(6,445)
445   FORMAT(//' 1:  PRINTOUT VALUES'/'  2:   RUN  PROGRAM
                 AGAIN')
```

```
          WRITE(6,450)
450         FORMAT('3:     PLOT   VALUES'/'4:     EXIT'//'ENTER
                     CHOICE',$)
          READ(5,460)PRE
460       FORMAT(A1)
          IF(PRE.EQ.'4')GO TO 301
          IF(PRE.EQ.'3')GO TO 800
          IF(PRE.EQ.'2')GO TO 300
          IF(PRE.EQ.'1')GO TO 660
          GO TO 440

C****** PRINT OUT VALUES ******
660       WRITE(6,670)
670       FORMAT('   TIME                 B'/28('-')/)
          DO 690 I=1,IMAX
          WRITE(6,680)TPRME(I),B(I)
680       FORMAT(F16.8,2X,F10.8)
690       CONTINUE
          GO TO 440

301       END
```

LIST OF REFERENCES

1. Jelley, J.V., Cerenkov Radiation and Its Applications, Pergamon Press, 1958.

2. Buskirk, Fred R. and Neighbours, John R., "Time Development of Cerenkov Radiation", Physical Review A, v. 31, Number 6, June 1985.

INITIAL DISTRIBUTION LIST

		No. Copies
1.	Defense Technical Information Center Cameron Station Alexandria, Virginia 22304-6145	2
2.	Library, Code 0142 Naval Postgraduate School Monterey, California 93943-5000	2
3.	Professor J.R. Neighbours, Code 61 Nb Department of Physics Naval Postgraduate School Monterey, California 93943-5000	4
4.	Professor F.R. Buskirk, Code 61 Bs Department of Physics Naval Postgraduate School Monterey, California 93943-5000	2
4.	Professor G.E. Schacher, Code 61 Sq Chairman, Department of Physics Naval Postgraduate School Monterey, California 93943-5000	2
5.	LCDR Kathleen M. Lyman, USN 129 Glascoe Avenue Staten Island, New York 10314	2

END

DTIC

10-86